PRONEURAL TRANSCRIPTION FACTOR NEUROD1-MEDIATED DIRECT NEURONAL REPROGRAMMING – AN AAV APPROACH

A THESIS

SUBMITTED TO THE FACULTY OF THE GRADUATE SCHOOL

OF THE UNIVERSITY OF MINNESOTA

BY

SWATHI RADHA

IN PARTIAL FULFILLMENT OF THE REQUIREMENTS

FOR THE DEGREE OF

MASTER OF SCIENCE

Dr. Walter C. Low

December 2019

ACKNOWLEDGMENT

I am extremely grateful to my advisor and mentor Dr. Walter C. Low for providing me with the opportunity to undertake my Master's thesis in his laboratory and his enthusiastic support and guidance through my thesis.

I express my heartfelt gratitude to my mentor Dr. Aleta R. Steevens, who has been a tremendous support and inspiration. Thank you for your patience and encouragement at every step of my project. I am sincerely thankful to all the members of the Low and Grande lab for building a nurturing and collaborative atmosphere.

I am deeply grateful to my mentor Dr. Susan Keirstead for her ever-enthusiastic moral and academic guidance and encouragement throughout my Master's program. A special thanks to my peers in the Stem Cell Biology program for their support and for making this journey enjoyable.

Lastly, I would like to thank my family and all my mentors who molded the person I am today. Thank you for all your wishes and encouragement to pursue my Master's degree in Stem Cell Biology at the University of Minnesota.

ABSTRACT

Direct cellular reprogramming to drive lineage switching from one differentiated cell type to another can be exploited to develop cell-based therapies for neurodegenerative diseases. *In vivo* reprogramming provides an attractive therapeutic strategy to circumvent the hurdles of immune rejection and ethical constraints associated with transplant-based therapy. Supporting glial cells of the CNS can be reprogrammed to neurons by targeted viral delivery of transcription factors and small molecules. Previous studies have demonstrated the effectiveness of a single proneural transcription factor NeuroD1 to drive reprogramming in the reactive glial lesions of Alzheimer's disease and stroke. However, the ability of NeuroD1 (ND1) to promote a similar benefit in models of Parkinson's disease (PD) has yet to be demonstrated.

The current study aims to test the hypothesis that NeuroD1 delivered via an Adeno-Associated Virus (AAV) can promote reprogramming in striatal astrocytes to neurons in an *in vivo* PD model. The FDA-approved, clinically employed AAV-9 gene delivery platform was used to transduce non-dividing cells with minimal off-target effects. A two-part AAV-9 viral system was designed to express ND1 in astrocytes, driven by the GFAP promoter. First, ND1-mediated direct neuronal reprogramming was tested using a simple and scalable *in vitro* culture system. Primary astrocytes *in vitro* transduced with the AAV9-ND1 dual virus system display characteristics of immature neuroglial precursor stage, suggesting successful reprogramming. Second, the potential of ND1 to drive reprogramming was assessed *in vivo* in mice. Intracranial and intravenously delivered AAV-9 dual virus system driven by the GFAP promoter targets astrocytes and surprisingly, mature resident neurons *in vivo*. Finally, ND1-mediated *in vivo* reprogramming was assessed in a well-established chemically-induced 6-hydroxydopamine (6-OHDA) Parkinson's disease mouse model. The 6-OHDA injury model provides insight into the novel application of the AAV-9 dual virus system to target astrocyte-to-neuron reprogramming as well as to target resident neurons for potential neuronal repair in Parkinson's disease.

TABLE OF CONTENTS

LIST OF TABLES

LIST OF FIGURES

CHAPTER I: INTRODUCTION

Direct neuronal reprogramming is an approach where ectopic expression of proneural transcription factors drives the switch in cell identity from terminally differentiated cell types, such as glial cells and fibroblasts, to neurons (Guo et al., 2014; Heinrich et al., 2014; Y. Liu et al., 2015). Using such an approach offers an attractive strategy to replenish neuronal populations lost in brain injury or neurodegenerative diseases of the Central Nervous System (CNS) such as Alzheimer's and Parkinson's disease. With the limited inherent regenerative capacity of the post-mitotic adult brain, *in vivo* reprogramming aims to convert endogenous supporting glial cells of the brain to neurons and contribute to a long-term functional benefit (Rivetti Di Val Cervo et al., 2017).

Current pharmaceutical interventions for neurodegenerative diseases alleviate symptomatic manifestations, however, they fail to address the permanent loss of neuronal populations. This deficit can be overcome by cell transplantation-based therapy to target potential long-term benefits (Chinta & Andersen, 2005). However, human fetal tissue-based allogeneic transplant therapy (Barker, Barrett, Mason, & Björklund, 2013) pose immune-rejection and ethical challenges. With the advent of induced Pluripotent Stem Cell (iPSCs) technology (Takahashi & Yamanaka, 2006), autologous cell-based therapy has opened up the possibility of deriving patient-specific iPSCs to generate differentiated cell types *in vitro*. Activation of key signaling pathways using small molecules or lineage-specific transcription factors have been identified to generate neuronal subtypes *in vitro* (Gascón, Masserdotti, Russo, & Götz, 2017). However, transplantation of the *in vitro* generated neurons poses a challenge for its functional integrating into the host circuitry. Additionally, the labor and time-intensive procedure to generate patient-specific iPSCs, followed by *in vitro* differentiation becomes impractical for acute therapeutic needs. Moreover, scaled-up production of the transplantable cells will be required to meet current clinical demands for transplantable cells (Goldman, 2016).

Direct neuronal reprogramming presents a novel cell replenishment approach for neurodegenerative diseases characterized by the extensive, irreversible loss of specific cell populations. One such progressive neurodegenerative condition is Parkinson's disease

(PD), manifested as a consequence of the loss of the midbrain dopaminergic neurons (mDA). The nigrostriatal pathway of the dopaminergic neurons affected in PD is composed of mDA axons projecting from the midbrain Substantia Nigra pars compacta (SNc) to the caudate-putamen in the dorsal striatum. Here, the neurotransmitter dopamine, released by mDA, signals the striatal medium spiny neurons (MSNs) and cortical and thalamic inputs to control motor function. Together, this system is involved in regulation and refinement of signals governing voluntary movement, achieved by the release of the neurotransmitter dopamine (Chinta & Andersen, 2005). The loss of dopaminergic neurons is manifested in the pathological features of PD, characterized by posture instability, muscle rigidity, tremors, and difficulty initiating voluntary movement (Parkinson, 2002).

The most common pharmaceutical intervention Levodopa (L-DOPA), administered orally as a tablet or capsule, is a dopamine precursor aimed to alleviate disease symptoms. This prodrug is enzymatically converted to functional dopamine in the CNS, thus, compensating for the decreased levels of endogenous dopamine. However, prolonged administration of L-DOPA is associated with adverse side effects, including nausea, but more importantly, the efficacy of L-DOPA decreases over time and it is not disease-modifying (Margolesky & Singer, 2018; Nagatsu & Sawada, 2009). Alternatively, *in vivo* reprogramming aims to provide long-term therapeutic intervention by replenishing dopaminergic neurons in order to achieve a functional benefit in PD.

Early approaches to direct neuronal reprogramming were inspired by iPSC technology. Potent neurogenic transcription factors such as Ascl1, Sox2, Neurog2, amongst others, were ectopically expressed in multiple cell lineages in an attempt to trigger a fate transition. Further, small molecules targeting key signaling pathways were demonstrated to enhance *in vivo* reprogramming efficiency (Hu et al., 2015; Ladewig et al., 2012; Li et al., 2015). A few major pathways targeted include inhibition of SMAD signaling, inhibition of BMP signaling using Noggin and enhancing neuronal survival and maturation using Brain-Derived Neurotrophic Factor (BDNF) (Niu et al., 2013). Additionally, permissive chromatin status that enables easy access to neuronal genes for the fate transition was proposed to improve reprogramming efficiency. Thus, Valproic acid (VPA), a histone deacetylase inhibitor has been employed to enhance chromatin

accessibility to facilitate successful initiation of the neuronal transcriptional program (Niu et al., 2013; Rivetti Di Val Cervo et al., 2017).

Three-dimensional chromatin structure along with defined epigenetic signatures preserved in terminally differentiated cell types can present a barrier to reprogramming (Gascón et al., 2017). According to the Waddington epigenetic landscape model, the terminal fate of a cell is determined by sequential genome modifications that branch it further away from its common shared progenitors (Waddington, 2014). Thus, identifying a cell source for neuronal reprogramming that possesses common developmental signatures can potentially ease the genetic barriers to reprogramming. Astrocytes, characterized to arise from the same common progenitor cells as neurons, are proposed as a potential cell source for reprogramming to ease this hurdle (Gascón et al., 2017).

Multipotent progenitor cells in the perinatal niches of the CNS have been identified to give rise to cells of both neuronal and glial lineage that diversify during the late development phase of the precursor cell (Goldman, Zukhar, Barami, Mikawa, & Niedzwiecki, 1996). While neurons form the primary signal processing units, astrocytes comprise the most abundant type of supporting glial cells. Tasked with the metabolic and functional support of neurons, astrocytes are integral to neuronal development and function. The stellate morphology of astrocyte aids in its close interaction with neurons, as well as the vasculature as a part of the blood-brain-barrier (BBB) (Oberheim et al., 2012).

Astrocytes have been demonstrated to respond to perturbation in the CNS, in the form of acute injury or progressive neurodegenerative diseases, as a player in the inflammatory response. Termed ‘reactive astrocytes’, they proliferate and migrate to the site of insult, forming glial lesions (Liddelow & Barres, 2017). Traditionally, associated morphological features of reactive astrocytes are an increase in the thickness and number of foot processes surveying the environment, as well as upregulated Glial Fibrillary Acid Protein (GFAP) (Eddleston & Mucke, 1993; Virchow, 1855). More recently, reactive astrocytes in the context of the inflammatory response and neurodegenerative conditions have been characterized to elicit a neurotoxic effect on neuronal function and survivability (Liddelow et al., 2017; Zamanian et al., 2012).

Thus, the abundance of astrocytes, along with their latent proliferative capacity makes them a promising potential cell source for reprogramming (Gascón et al., 2017). Furthermore, the strategy to convert astrocytes to neurons *in vivo* serves a dual-pronged approach: As a primary objective, neuronal populations lost in the context of injury or diseases can be replenished to confer a functional benefit. As a secondary benefit, neurotoxic astrocytes in the glial lesions can be eliminated (Guo et al., 2014).

Various approaches have been identified to target *in vivo* reprogramming. Particularly, the ectopic expression of proneural transcription factors such as Sox2, Ascl1, and Lmx1a in fibroblast and glial cells have been demonstrated to induce direct neuronal reprogramming with varying degrees of efficiency (Caiazzo et al., 2011; Grande et al., 2013; Heinrich et al., 2014; Y. Liu et al., 2015; Niu et al., 2013). One such proneuronal transcription factor is the basic Helix-Loop-Helix (bHLH) protein Neurogenic Differentiation factor 1, NeuroD1 (ND1). Detected first during early mouse embryonic development at E9, the expression of ND1 was largely restricted to proliferating neural precursor cells that just exited the cell-cycle, suggesting a lineage commitment role (Cho & Tsai, 2004; Ma, Kintner, & Anderson, 1996). The potent neurogenic potential of ND1 was demonstrated when the ectopic expression of the gene promoted premature neuronal differentiation in *Xenopus* developing embryo (J. E. Lee et al., 1995). Further, homozygous knockout mice lacking stable expression of ND1 in the adult brain, exhibited severe neurological and auditory defects, thus revealing its role in the survival and maintenance of neuronal cells (Z. Gao et al., 2009; M. Liu et al., 2000).

Emerging evidence attributes the reprogramming capability of ND1 to its role as a pioneer factor, a transcription factor that can directly bind condensed chromatin (Zaret et al 2011). By binding to transcriptionally repressed regulatory elements, ND1 enhances chromatin accessibility to facilitate the binding of co-regulatory factors required to initiate reprogramming (Matsuda et al., 2019). Key amongst these co-regulatory factors are the epigenetic modifier proteins such as the Polycomb-group and MBD3, which are involved in propagating active or repressive epigenetic signatures in neuronal lineage specification (Pataskar et al., 2016).

Collectively, the developmentally critical role of ND1 in neuronal lineage specification as well as in neuronal differentiation and maturation makes it a prime candidate for reprogramming. Guo et al., (2014) demonstrated that the retrovirus-mediated forced expression of ND1 converted reactive astrocytes to glutamatergic neurons in mouse models of stab-wound injury as well as Alzheimer's disease.

In vitro direct neuronal reprogramming to obtain dopaminergic neurons lost in PD was demonstrated by Rivetti Di Val Cervo et al., (2017). Lentivirus was used to deliver a combination of three proneural transcription factors, NeuroD1, Ascl1, and Lmx1a along with a microRNA – mi218, collectively referred to as NeAL218, to induce the fate transition. Improved *in vitro* reprogramming with NeAL218 was observed in the presence of small molecules such as a dual-SMAD inhibitor as well as midbrain specific patterning signals. Brief initial exposure to chromatin remodeling agents such as Valproic Acid (VPA) and 5-aza-2'-deoxycytidine (Dec) also seemed to enhance reprogramming efficiency (Rivetti Di Val Cervo et al., 2017). The NeAL218-mediated reprogramming was recapitulated *in vivo* in mice using a 6-hydroxydopamine (OHDA) induced Parkinson's mouse model. Newly reprogrammed dopaminergic neurons in the striatum showed functional features of healthy neurons, as well as contributed to a functional benefit in the behavioral recovery of motor functions in the mouse model (Rivetti Di Val Cervo et al., 2017).

The reprogramming field thus far has employed a retrovirus or lentivirus-based delivery of proneural genes. Enveloped retrovirus with a 7-9kb single-stranded RNA (ssRNA) genome exhibits a high potency of transducing mitotically active cells (Brown, Bowerman, Varmus, & Bishop, 1987). In comparison, the lentivirus system can package up to a 10-11kb genome with the ability to transduce both dividing and non-dividing cells. Long-term stable expression of viral genes in the host cell is achieved by the integration of the reverse transcribed double-strand DNA (dsDNA) (Naldini, 1998; Warnock, Daigre, & Al-Rubeai, 2011).

Although retrovirus vectors exhibit a high transduction efficiency, integration of viral genes into the host genome poses a high risk of off-target effects. Random integration is often accompanied by silencing or disruption of functional genes (Baum, 2007). Further,

retrovirus can also initiate strong immune responses that diminish the potential clinical application of these vectors.

By contrast, the Adeno-Associated Virus (AAV) is a class of non-pathogenic helper-dependent viruses that can target both dividing and non-dividing cells. Flanked by Inverted Terminal Repeats (ITR) required for viral replication and packaging, the genome contains two open-reading frames (ORFs) that encode the Replication gene (*Rep*), which is required for the AAV life cycle, and the capsid protein (*Cap*). In a gene delivery vector, the *Rep* and *Cap* genes are replaced by an artificial promoter-gene sequence (Deyle & Russell, 2009; Ellis et al., 2013). Although limited in its packaging capacity (4.7kb), the ssDNA genome of AAV forms concatamers that are expressed episomally in transduced cells. A small percentage of the AAV genome has also been shown to integrate at a specific locus on chromosome 19, termed AAVS1 site, however, without any extensive off-target effects (McCarty, Young, & Samulski, 2004; Schnepp, Jensen, Chen, Johnson, & Clark, 2005). AAV has also been demonstrated to elicit a minimal immune response, thus, has been approved by the Food and Drug Administration (FDA) for clinical applications for diseases of the CNS (Lykken, Shyng, Edwards, Rozenberg, & Gray, 2018; Naso, Tomkowicz, Perry 3rd, & Strohl, 2017).

To date, numerous distinct strains or serotypes of the AAV have been isolated (G. Gao & Wilson, 2005). Characterization of the AAV virus further led to the identification of serotypes with preferential cell- and tissue-type specificity, defined as tropism. One such serotype, AAV9, exhibits tropism selectively to neurons and astrocytes in the CNS, making it a valuable gene delivery vector (Schuster et al., 2014; Zincarelli, Soltys, Rengo, & Rabinowitz, 2008). Multiple lines of investigation have identified the ability of AAV9 to cross the blood-brain-barrier and preferentially transduce neurons and astrocytes (Foust et al., 2009; Merkel et al., 2017; Zhang et al., 2011).

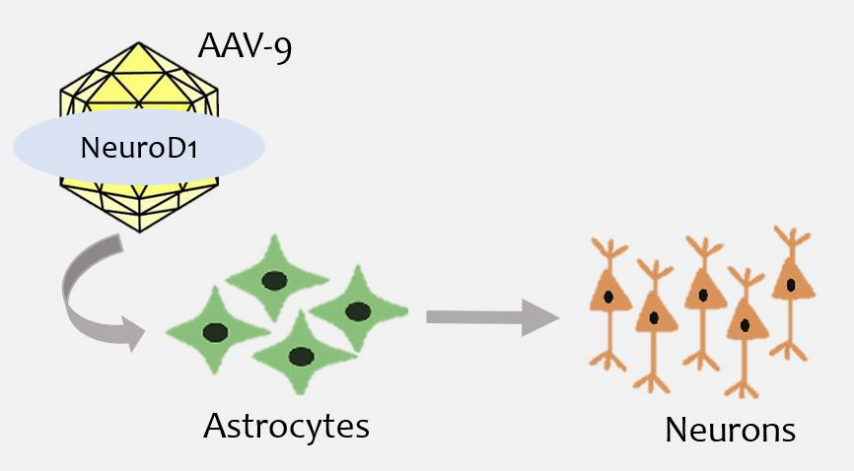

Figure 1: *Strategy for direct neuronal reprogramming*

In summary, viral vector-mediated ectopic expression of proneural transcription factors has been demonstrated to drive the reprogramming of supporting cells of the brain to neurons in various contexts of brain injury.

The current work tests the hypothesis that the proneural transcription factor NeuroD1 has the ability to drive direct neuronal reprogramming *in vivo* in a Parkinson's disease mouse model. To develop a clinically translatable approach, the Adeno-Associated Virus AAV-9 was used as a gene delivery platform (**Figure 1**). To achieve targeted expression in astrocytes, a dual plasmid approach was designed: one expressing the Cre recombinase, driven by an astrocyte-specific GFAP promoter and the second reporter construct with CAG::DIO-mRuby2 as control or a CAG::DIO-NeuroD1-P2A-mRuby2 reprogramming virus. The double-inverted flox (DIO) site allow for the Cre-dependent constitutive expression of the reporter mRuby2 and ND1 under the CAG promoter. First, the potential of AAV-9-mediated NeuroD1 to convert astrocytes to neurons was assessed using an *in vitro* astrocyte culture system. Next, the potency of NeuroD1 to drive reprogramming *in vivo* in the striatum of adult mouse was interrogated. Additionally, to identify a viral delivery mode to efficiently target astrocytes, intracranial and intravenous AAV-9 injections were performed. Finally, the reprogramming ability of AAV-9-delivered NeuroD1 was tested in the context of Parkinson's disease using the 6-hydroxydopamine (6-OHDA) Parkinson's disease mouse model.

CHAPTER II: METHODS

SECTION 1: *In vitro* reprogramming

NeuroD1-mediated direct neuronal reprogramming was first tested in an *in vitro* culture system in order to create a simple and scalable reprogramming system. Primary astrocytes were chosen to establish the culture system, as they provide a better representation of the *in vivo* biology as compared to commercially available cell lines. This section describes the methodologies for the isolation and purification of primary mouse astrocytes, characterization of the culture system and Adeno Associated Virus, AAV-9 transduction with dual virus system to assess NeuroD1-mediated reprogramming of astrocytes *in vitro*.

1. Isolation of primary mouse astrocytes

Cortical astrocytes in the developing mouse brain at the post-natal age of P0-P4 are in an immature state, thus possess a high proliferative capacity, and can be expanded and maintained in culture. The basic principle for the isolation and purification of astrocytes follows a twofold approach. First, astrocyte growth media is formulated with a high glucose concentration (5.5g/L) and serum to support the growth of glial cells. Neurons in the culture are eliminated based on the lack of key supplements such as B27 and N2 and neurotrophic growth factors such as EGF and FGF. Second, constant vigorous shaking for 6 hours purifies astrocytes from the mixed glial culture. This step selects for the astrocyte population that exhibits robust attachment to the cultureware, a property not exhibited by microglia and oligodendrocytes. Primary astrocytes obtained from a maximum of three passages were used for the *in vitro* reprogramming experiments as suggested by Schildge, Bohrer, Beck, & Schachtrup (2013).

P0 mouse pups were decapitated and the cranial flaps gently peeled open to expose the brain. The brain was removed from the skull and immediately transferred to 1ml cold 1X Hank's Balanced Salt Solution (HBSS) (Thermo Fisher Scientific, Cat.# 14175095) on a 35mm Petri dish (CytoOne, Cat.# CC7682-3340) and placed on ice. The olfactory bulbs and cerebellum were detached and removed leaving behind the cortices and associated mid-brain regions. Meningeal tissue marked by capillaries was gently peeled away to

eliminate meningeal cells and fibroblasts from the culture. 0.25% Trypsin solution (25 N.F. U/mg) (Thermo Fisher Scientific, Cat. # 15090046) was added to the 35 mm plate with the isolated cortices, which were then minced into smaller bits. Four mouse brains, estimated to yield $1*10^6$ cells, were pooled together to be seeded in a single T-75 flask (Olympus Plastics, Genesee Scientific, Cat.# 25-209) (Schildge et al., 2013). The tissue with 0.25% Trypsin solution was incubated at 37° C for 30 min. HBSS was added to the dissociated tissue and centrifuged for 5 min at 1500 rpm to remove the Trypsin. Aspirated supernatant was discarded and pre-warmed astrocyte growth media (**Page 10**) was added to resuspend the tissue clumps. Vigorous trituration was done using a micropipette to homogenize the tissue clumps into a single cell suspension. Cell number and viability were quantified using a hemocytometer and Trypan blue that stains for dead cells(Sigma-Aldrich, Cat.# 72-57-1) staining. The cell suspension was added to pre-coated T-75 flasks and incubated at 37° C with 5% CO_2, to be used for the *in vitro* experiments.

2. Pre-treatment of cultureware

To facilitate attachment of astrocytes to the culture flask, the growth surface was coated with Poly-l-Lysine (PLL), a synthetic homopolymer, whose surface residues provide anchorage points for the astrocytes. PLL is a bio-compatible cationic molecular coating agent that facilitates attachment of the negatively charged cell membrane by electrostatic forces (Mazia, Schatten, & Sale, 1975).

T-75 flasks (Corning, Cat.# CLS430639) were freshly coated with 1X PLL right before seeding the astrocytes. PLL at a working concentration of 50 µg/ml (1X) was added to the T-75 flask and incubated at 37° C for 1 hour to ensure even coating. PLL was discarded and 1X Phosphate Buffered Saline (PBS) (GeneSee Scientific, Cat.# 25-507B) was added to thoroughly wash the flask, followed by a second wash to remove remaining traces of PLL. Astrocyte growth media pre-warmed to 37 °C was added to the flask before seeding the cells. A similar procedure was followed to coat the well-plates and chamber slides.

3. Astrocyte culture media

1. High glucose Dulbecco's Modified Eagle Media (DMEM) – 5.5g/L D-Glucose
2. Penicillin/Streptomycin – 10,000 units/ml each (1% final concentration)
3. Heat Inactivated Fetal Bovine Serum (FBS) – 10% final concentration

High glucose DMEM (4.5g/L D-Glucose, Thermo Fisher Scientific, Cat.# 11965084), with Sodium Pyruvate, Calcium and Magnesium was used for the astrocyte growth media, supplemented with additional glucose to make the final glucose concentration of 5.5g/L (Sigma-Aldrich, Cat.# G7021). Antimicrobial-antifungal agents such as Penicillin-Streptomycin (Thermo Fisher Scientific, Cat.# 15070063) were added (1% final concentration) to prevent contamination of the culture. Heat-inactivated FBS (GeneSee Scientific, Cat.# 25-514H) was added to the media to provide the growth factors required for astrocyte growth and development. Heat-inactivation of FBS denatures the complement proteins that could otherwise elicit an immune-responsive environment in the culture system (Soltis, Hasz, Morris, & Wilson, 1979; Triglia & Linscott, 1980).

4. Purification of Astrocytes

Mixed glial cells in the culture are separated based on the adherence properties of different glial cells. While astrocytes strongly adhere to the surface, superficial microglia and oligodendrocyte precursor cells (OPCs) and oligodendrocytes are detached when the culture is shaken vigorously (Schildge et al., 2013).

The mixed-glial cells in T-75 flasks on day 7 were agitated using an orbital shaker (GeneMate OS350) at a constant speed of 180 rpm for 30 min to remove the superficial microglial layer. The culture flask along with the orbital shaker was maintained throughout in the incubator (CEDCO©) at 37° C, supplied with 5% CO_2. The supernatant containing the detached microglia was cultured to validate the purification step. Fresh Astrocyte Media was added to the flask and agitated for 4 hours at 240 rpm, followed by additional tapping to enhance the detachment of OPCs and oligodendrocytes. The supernatant containing the OPCs was separated and retained for culture. Following a wash step with PBS, the astrocyte monolayer was detached by treatment with 0.25% Trypsin solution at 37° C, with 5% CO_2. Media was added to neutralize the Trypsin and the cell suspension

was centrifuged at 1500 rpm for 10 min at 21° C. Anti-trypsin proteins in the serum deactivate trypsin and prevent excessive cellular damage (Bundy & Mehl, 1959). Supernatant was discarded and the cell pellet was resuspended in culture media to quantify cell number and viability with Trypan Blue using a hemocytometer. Approximately $1*10^6$ cells were added to a pre-coated T-75 flask and the culture was expanded *in vitro* or cryo-preserved for future experiments.

5. Cryopreservation of astrocytes

Freeze media composition

1. Fetal Bovine Serum (FBS) – 90%
2. Dimethyl sulfoxide (DMSO) – 10%

Astrocytes after a single passage were expanded in culture until reaching approximately 100% confluency. For long-term storage, astrocytes were cryo-preserved. Since cryo-preservation involves storing biological samples in liquid nitrogen at an extremely low temperature of -196° C, cryo-protectant agents prevent the formation of ice crystals when the cell suspension is rapidly cooled (Jang et al., 2017). To preserve the cell viability, phenotype, and minimize damage or degradation of the astrocytes, DMSO was used as a cryo-protectant (Best, 2015; Notman, Noro, O'Malley, & Anwar, 2006).

Astrocyte culture was incubated with 0.25% Trypsin solution (25 N.F. U/mg) for 1 min at 37° C and 5% CO_2. The flask was vigorously tapped to ensure complete dissociation and detachment. Media was added to neutralize trypsin and the cell suspension was centrifuged at 1500 rpm for 10 min at 21° C. Supernatant was discarded and the cell pellet was gently resuspended in media to quantify cell viability as done previously. Pre-chilled cryopreservation media with 90% FBS and 10% DMSO (Sigma-Aldrich, Cat.# D2650) was added to the cell suspension and transferred to a cryovial, with each vial having 1ml cell suspension that is estimated to have approximately 1 million cells. Vials were frozen at -80 °C in freeze-containers designed to regulate the freezing rate at 1° C/min. For long-term preservation, the cryovials were stored in liquid nitrogen at -196° C.

6. *Thawing frozen astrocytes for culture*

Thawing cryopreserved cells is crucial to ensure cell viability and functions. In contrast to the gradual cooling rate maintained while freezing down cells (-1°C/min), rapid warming yields the best results while thawing astrocytes (Yokoyama, Thompson, & Ehrhardt, 2012).

Cryovial stored in liquid nitrogen was transferred to a water bath at 37 °C and gently swirled until only a small ice crystal remained. The cell suspension was added to pre-warmed media and centrifuged at 1500 rpm for 10 min at 21° C to remove the DMSO. The cell pellet was resuspended in fresh pre-warmed media to quantify cell number. The astrocyte cell suspension was added to a coated T-25 flask with pre-warmed media.

7. *Design of Viral Vector Constructs*

The design for the dual virus system for Control and Reprogramming gene constructs was conceptualized by Post-Doctoral Fellow Dr. Aleta R. Steevens in the Low lab, in collaboration with Dr. Ezequiel Marron at the Department of Pharmacology and Viral Vector and Cloning Core, University of Minnesota, Twin Cities.

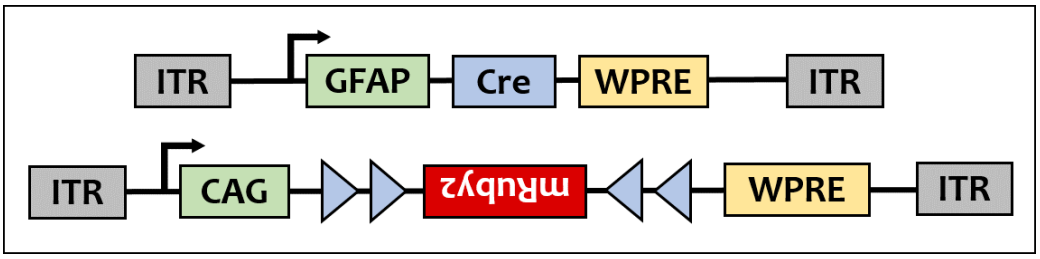

Figure 2: *Control Dual virus system. GFAP – Glial Fibrillary Acid Protein, Cre – Cre recombinase, WPRE – Woodchuck Post-Transcriptional Regulatory Element, ITR – Inverted Terminal Repeats, CAG – CMV enhancer fused to chicken β-actin promoter.*

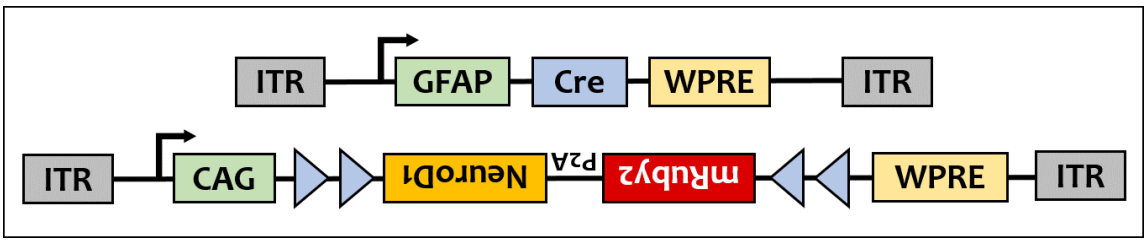

Figure 3: *ND1-Reprogramming dual virus system*

Targeted expression of NeuroD1 (ND1) in astrocytes was obtained using the genetic strategy of Cre-lox recombination. The expression of Cre recombinase is driven by the GFAP promoter in the first construct. Glial Fibrillary Acidic Protein (GFAP) is a structural protein established to be expressed in astrocytes (Eng, Vanderhaeghen, Bignami, & Gerstl, 1971; Lewis, Balcarek, Krek, Shelanski, & Cowan, 1984).

The second construct is designed to express the red fluorescent reporter, mRuby2, under the ubiquitous CAG promoter. The inverted orientation of the reporter sequence within double-inverted flox (DIO) sites positions the reporter in the antisense (OFF) orientation. This allows for the expression of reporter only in the presence of Cre, which recognizes the dual flox sites and inverts the intervening genetic contents between the flox sites into the sense (ON) orientation (Atasoy, Aponte, Su, & Sternson, 2008). To enhance the expression of the viral constructs, the post-transcriptional regulatory element (WPRE) is encoded at the 3' end (Higashimoto et al., 2007; Loeb, Cordier, Harris, Weitzman, & Hope, 1999).

Using a similar strategy, the reprogramming construct encodes the sequence for the proneural gene NeuroD1 linked to the reporter mRuby2 within the DIO sequences, in the same plasmid backbone. The short P2A linker sequence enables the transcription of both NeuroD1 and mRuby2 sequences in the same transcript as well as co-translation in the same frame. Thus, mRuby2 serves as a lineage tracing tag in cells transduced with the dual virus system (Trichas, Begbie, & Srinivas, 2008).

The combination of the GFAP-Cre constructs with the CAG-mRuby2 forms the Control system (**Figure 2**) while GFAP-Cre with the NeuroD1-mRuby forms the Reprogramming system (**Figure 3**). The plasmid backbones and vector constructs were obtained from AddGene and packaged by Dr. Marron at the virology core at the University of Minnesota.

8. In vitro Viral Transduction

To investigate NeuroD1-mediated reprogramming *in vitro*, astrocytes in culture were transduced with the AAV-9 control and reprogramming dual virus system. To promote efficient transduction, a high Multiplicity of Infection (MOI) of 80,000 or 160,000 was used (Aschauer, Kreuz, & Rumpel, 2013; Ellis et al., 2013). The MOI (total number of

viral particles transducing a single cell) and estimated astrocyte density in culture were used to calculate the viral titers required for infection, shown in **Appendix II**. The viral solution was suspended in pre-warmed media and added to the well-plate/chamber slides and incubated for 24 hours at 37 ° C and 5% CO_2. 24 hours post-transduction, media containing the virus particles was removed and subsequent media changes were done every 2-3 days. 7 days post-transduction, the culture was processed for Immunocytochemistry (ICC) analysis.

SECTION 2: *In vivo* reprogramming

While the *in vitro* system enables a straightforward mechanistic assessment of reprogramming, it fails to capture the in-vivo cellular environment that can influence direct reprogramming (Grande et al., 2013). Thus, ND1-mediated reprogramming was tested *in vivo* in a murine model. This section describes the methodologies to assess AAV-9 delivery strategies using either intracranial and intravenous injection and test reprogramming in a pilot model of 6-OHDA Parkinson's Disease (PD) mouse model, followed by isolation and processing of whole brain tissue for analysis.

1. Intracranial Viral Delivery

With the goal of reprogramming striatal astrocytes, viral vectors for the control and reprogramming constructs were directly injected at the striatum using a stereotaxic surgical setup.

Intraperitoneal injection of sustained-release Buprenorphine (1µl/g body weight, ZooPharm Pharmacy) was administered 2 hours prior to the start of surgery. Inhalable Isofluorane (Piramal Critical Care Inc., NDC# 988015) at a concentration of 2.5% in oxygen was used to anesthetize the mice in a closed chamber. Toe pinch reflex was done to assess anesthetic depth before positioning the mouse onto the stereotaxic frame (KOPF®, 900LS) fitted with heating pads to maintain the body temperature. The head was centered and secured firmly using ear bars that were positioned at the lateral skull grooves through the ear canal. The nose cone was positioned to supply inhalable isoflurane and prevent rotational movement of the mouse head. Following removal of the fur, the scalp was disinfected using alcohol swabs (Covidien, Cat.# KN6818) and antiseptic Betadine

solution (Providone-Iodine solution, Aplicare, Cat.# 82226). Hydrating sterile eye gel drops (Sunmark, NDC# 49348-947) was applied to the eyes to prevent drying and formation of corneal ulcers. A midline sagittal incision through the scalp was done to expose the skull. Coordinates for the striatum were measured from the anatomical reference point, Bregma, identified as the intersection of the sagittal and coronal sutures on the skull. A 26-gauge Hamilton syringe (Hamilton ®, Model# 701) loaded with the viral solution was positioned at the Bregma point and the Vernier scale was used to measure the coordinates along the Anterior/Posterior (A/P), Medial/lateral (M/L) and Dorso/Ventral (D/V) axes. The needle was repositioned to the target coordinates with respect to bregma for the striatum: (A/P): +1.0mm, and (M/L): -1.5mm as determined using the Allen Mouse Brain Atlas (Paxinos & Watson, 2006). The target site on the skull was marked using a pencil. A Burr hole was drilled at the marked spot using 0.9mm drill-bit (Dremel, Model# 8050-N/18) through which the syringe was inserted and lowered to the target injection site coordinates along the D/V axis: -3.25 for the first more ventral injection and -2.5mm for the second more dorsal injection. An automated pump was used to inject a total of 3 µl of the AAV-9 viral solution to ensure precise, controlled and uniform distribution of the viral particles at the striatum. The automatic injector was switched on to inject the solution at a speed of 500 µl/min. The needle was retained at the site for 5-10 min after the injection to ensure even diffusion of the solution. The needle was then slowly withdrawn and cleansed with a Micro-90 solution, deionized water, and Acetone, following that order, before re-using it for a second injection. Skin from both sides of the incision was stapled together or sutured to close the incision. Mice were transferred to their cage which was placed on a heating pad and provided with moistened chow.

Following recovery from the anesthesia, about 1/2 hour after surgery, mice were assessed for alertness, movement activity as an indication of a healthy recovery from surgery. Mice were housed in the Research Animal Resources (RAR) Facility and post-operative examination of weight, activity status, dehydration was monitored for the following 3 days. Mice exhibiting weight loss of >1.5g/day and dehydration were administered sterile saline (Bacteriostatic sterile 0.9% saline, Hospira Inc., Cat.# 236173) intraperitoneally. Completely healthy and recovered mice displayed active mobility, alert responses to stimulus and a shiny well-groomed fur, a typical response noted post-surgery.

2. Tail Vein Injection

AAV-9 tail vein injection was done to examine the cellular tropism of the virus based on delivery mode. Foust et al. (2009) demonstrated AAV-9 to preferentially transduce neurons co-labeled with NeuN, in the CNS when injected intracranially. However, AAV-9 when delivered through intravenous route to adult mice, predominantly transduced astrocytes in the CNS, co-labeling GFAP+ cells.

To determine the optimal route of targeted viral delivery best suited to target astrocytes, AAV9-GFAP::Cre was injected into an Ai9-tdT reporter mouse strain that is genetically engineered to express a reporter tdTomato (tdT) only in the presence of Cre recombinase. The LoxP-flanked STOP sequence encoded upstream of the reporter is excised by Cre recombinase, thus, expressing tdT under the ubiquitous Rosa promoter in cell types with Cre expression. This experiment serves as an important control as it will determine what cell type the viral system is capable of transducing. Expression of the reporter tdT was anticipated to be observed in AAV9-transduced cells with GFAP-promoter activity i.e. astrocytes. Tail vein injections were performed by Nicole Emmitt, a graduate student from the Low and Cheeran lab.

A restraining apparatus was used to restrain the mouse and allow unhindered access to the tail. Following disinfection with ethanol swabs, the tail was briefly exposed to a heat lamp to engorge the veins for ease of injection. 100µl solution containing $4.5*10^{11}$ GC/µl was injected into the tail-vein using a 26-gauge needle. The needle was left in place for a few extra seconds before withdrawing to prevent the virus solution from leaking. The tail was swabbed with an alcohol pad after removing the needle and the mice were returned to their cage.

3. 6-OHDA Parkinson's disease mouse model

To test the efficiency of NeuroD1-mediated *in vivo* reprogramming in the context of a neurodegenerative brain injury, a Parkinson's disease mouse model was chosen. The neurotoxin, 6-hydroxydopamine (6-OHDA), was used to establish the well-validated chemically induced model of Parkinson's disease. Previous studies have demonstrated the efficiency of 6-OHDA to model PD by targeted ablation of dopaminergic neurons that is

mediated by mitochondrial dysfunction and oxidative damage. This model was chosen for its ability to reproduce the molecular and behavioral features of the parkinsonian phenotype. In addition, 6-OHDA is unable to cross the blood-brain-barrier, thus, ensuring safety to researchers (Tieu, 2011).

As a pilot experiment, 6-OHDA-HCl (Sigma-Aldrich, Cat.# 28094-15-7) intracranial delivery in adult mice (aged >7weeks) was performed following the methodologies described by (Rivetti Di Val Cervo et al., 2017). The injection was targeted at the axons of the dopaminergic neurons, termed the Medial Forebrain Bundle (MFB), with the coordinates: A/P: -1.2, M/L: -2.0, and D/V: -4.8, identified according to the Allen Mouse Brain Atlas. 1µl of 6-OHDA (3.75µg) was intracranially injected, following the protocol mentioned above. Recovery from surgery and post-operative preliminary health status of the mice were monitored for three days following surgery as described before. All procedures were performed according to the guidelines established by the University of Minnesota Institutional Animal Care and Use Committee (IACUC).

4. Intracardial perfusion to fix the whole brain

Whole-brain was isolated for analysis. To fix and preserve the structural and molecular characteristics of the intact brain, the fixative agent 4% paraformaldehyde was intracardially perfused. Perfusion through the natural vasculature removes the blood and allows the fixative to permeate deep into the tissue and preserve the physiological characteristics of the tissue. Optimum fixation is critical to identify and localize cellular protein expression using Immunohistochemistry (IHC) (Gage, Kipke, & Shain, 2012).

Mice were anesthetized using isoflurane, delivered with oxygen at a concentration of 2.5% and maintained at a rate of 1.5 L/min. Toe pinch reflex was monitored to assess anesthetic depth. Precise incisions were performed to open the abdomen cavity, remove the diaphragm, thus exposing the heart and lungs. Extra fibrous tissue lining the heart was carefully peeled away and a 26-gauge needle was inserted through the tip of the left ventricle to deliver the perfusate. The right atrium was snipped as an outlet for the circulated solution. To maintain the controlled and uniform pressure of the perfusion solution, a mechanical pump was employed. Mice were first perfused with ice-cold PBS to flush out the blood from the circulatory system. The endpoint was indicated by a distinct

change in the color of the liver, from the natural deep red to yellow. Ice-cold 4% paraformaldehyde (PFA) (Alfa-Aesar, Cat.# A11313-36) was injected to fix the tissues, the end-point indicated by stiffened limbs and organs. To isolate the brain, mice were first decapitated skin peeled away to reveal the skull. Precise incisions were made to remove the brain from the cranium. The brain was transferred to a chilled 4% PFA solution and incubated overnight to enable complete tissue fixation.

5. Post-fix processing of brain tissue

Fixed whole brains were put through a sucrose gradient as a cryoprotectant, to remove water prior to freezing and to preserve tissue integrity for long-term preservation. Following overnight incubation with 4% PFA, the whole brain was washed thrice with cold PBS, for 15min each, to remove traces of PFA completely. The tissue was transferred to a 10% sucrose (Fisher Scientific, Cat.# 57-50-1) solution and incubated overnight at 4° C. Tissue equilibrated with the sucrose solution was indicated by the brain sinking to the bottom of the tube. A similar treatment step was followed for 20%, followed by a 30% sucrose solution. Tissue was then equilibrated and embedded in Tissue Freezing Media (TFM) (General Data Inc., Cat.# TFM-5), a quick-freeze solution that provides structural support for the tissue for cryotomy and prevents crystallization. Tissue was positioned in the desired orientation into the tissue embedding molds (Thermo Scientific) and was snap-frozen by placing on dry ice (-80 °C). For long-term storage, embedded tissues were stored at -80 °C.

6. Cryosectioning

For Immunohistochemistry (IHC) analysis of the striatum within the whole brain, cryopreserved brain tissue was coronally sectioned to visualize both the ipsilateral and contralateral hemispheres of the brain (**Figure 4**).

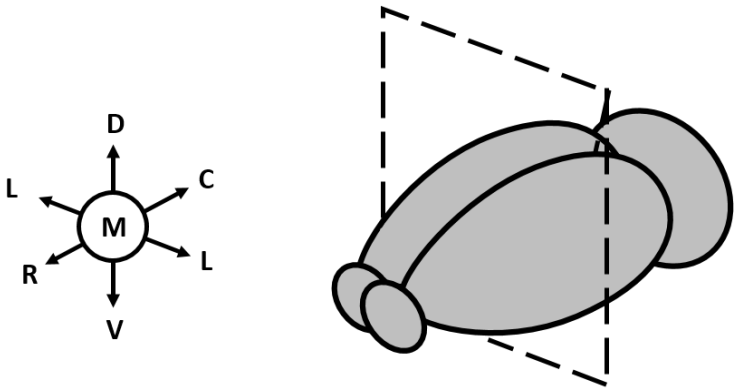

Figure 4: *Illustration representing the coronal sectioning plane for mouse brains. R – Rostral, C-Caudal, M, Medial, L- Lateral, D – Dorsal, V - Ventral*

Brains embedded in TFM were secured onto the cryosectioning chuck using the Optimum Cutting Temperature (OCT) compound (Fisher HealthCare, Cat.# 23-730-571) and sectioned at a thickness of 20 microns on the Leica Cryostat equipment (Leica, Model# CM1860). A temperature range of -27° C to -21° C was maintained to prevent curling or crumpling of the tissue. Slides with directly mounted sections were dried for 30 min on a slide warmer, followed by long-term storage at -20° C (Fischer, Jacobson, Rose, & Zeller, 2008).

7. Immunohistochemistry/Immunocytochemistry

To detect the presence and localization of fluorescent reporter protein as well as the endogenous cell-type-specific proteins, indirect immunohistochemistry was performed.

Slides with the pre-mounted sections were warmed for 30 min on a slide warmer. The slide edges were lined with a hydrophobic Super^{HT} PAP-pen (Research Products International Corp., Cat.# 195505) to retain the staining solutions within the slide. Sections were post-fixed with 4% PFA (Santa Cruz Biotechnology Inc., Cat.# 30525-89-4) for 5 min to enhance firm attachment to the slide. PBS was used to wash off the PFA. This was followed by a detergent-based wash using PBS + 0.1% Triton X-100 solution (Fisher Scientific, Cat.# 9002-93-1). The wash step was repeated twice for 15 min each at RT. Brain sections were then treated with a strong detergent-based J-Block solution to permeabilize cell membranes, thus enhancing the stringency of antibody binding (**Table 1**). The J-block

solution with Bovine Serum Albumin (BSA) (ICN Biomedicals Inc.) was added to sections and incubated for 10 min at RT.

	Components	***Concentration***
1.	Triton X-100	1.0 %
2.	Bovine Serum Albumin	1.0 %

Table 1: *Composition of J-Block solution*

To prevent the binding of antibodies at non-specific sites, sections were incubated in a blocking solution. Sections were incubated in PHT-block solution (PBST + Horse serum + Triton + BSA) (**Table 2**) for 45min-1 hour at RT. Serum and BSA are common blocking agents that prevent electrostatic binding of staining antibodies to charged protein residues in the tissue, thus, eliminating non-specific/background staining in IHC (Boenisch, 2001).

	Components	***Concentration***
1.	Triton X-100	0.3 %
2.	Bovine Serum Albumin	1.0 %
3.	Horse Serum	10 %

Table 2: *Composition of PHT-blocking solution*

Primary antibodies diluted in blocking solution were added to the sections and incubated overnight at 4 °C. Different host species each of the primary antibodies were chosen in a single staining combination to prevent cross-reactivity with the secondary antibodies (**APPENDIX III: Antibodies for IHC/ICC**). To check for the specificity of secondary antibodies, control samples were treated only with secondary antibody in the absence of primary antibodies. PBS as wash solution was added to the sections and incubated for 30 min at RT. Further staining procedure was carried out in the dark to prevent photo-bleaching of the fluorescent molecules tethered to the secondary antibodies. Secondary antibodies corresponding to the host species of the primary antibodies were diluted at a dilution rate of 1:1000 in PHT-block solution. DAPI was used as a counterstain to mark cell nuclei. DAPI (Invitrogen, Cat.# D1306) at a working concentration of 1µg/ml

was mixed with the secondary antibody solution. Samples were incubated in the secondary antibody solution for 2 hours at RT. To remove unbound secondary antibodies and DAPI, sections were washed three times with PBS for 15 min each rinse at RT. Wash solution was discarded and a few drops of Immu-mount mounting solution (Thermo Scientific) were placed on the slide. Coverslip was positioned carefully over the sections, ensuring no bubbles were formed. The excess mounting solution was wiped off the slide edges and sealed tight using a sealant. Slides were air-dried in the dark before storing at -20° C for long-term preservation.

8. Microscopy

IHC-based protein expression in fixed cells and brain tissue sections was visualized and imaged on the Leica Inverted epifluorescence microscope system (Leica DMi8). Fluorescence intensity for each of the fluorophore was calibrated to ensure optimum data read-out for each of the four fluorescent emission wavelengths. Adjusted exposure time was appropriately set to avoid over-exposing or under-exposing the sample.

9. Image Analysis using ImageJ

Analysis of the acquired images was done using ImageJ, an open-source image processing program developed at the National Institutes of Health (Rasband, W.S., ImageJ, U. S. National Institutes of Health, Bethesda, Maryland, USA, https://imagej.nih.gov/ij/, 1997-2018). Quantification of the data was performed by using the cell-counter tool. Scale bars at each magnification were calibrated using the stock scale bar through the Leica microscope software. Figures were prepared using ImageJ and Microsoft PowerPoint.

CHAPTER III: RESULTS

SECTION 1: *In vitro* Reprogramming

1. Isolation and Culture of primary astrocytes

Astrocytes from the mixed glial culture were purified based on their strong adherence to the culture flask compared to microglia and Oligodendrocyte Precursor Cells (OPCs). 7 days after plating the isolated primary mixed glial cells, the T-75 flask was agitated at a constant speed for 30 min to remove the microglial population attached to the astrocyte monolayer. Further agitation for 6 hours resulted in the detachment of the OPCs and oligodendrocytes. The supernatant containing the detached cells was centrifuged and the resuspended cells were plated for culture in astrocyte growth media (**Figure 5**). The anticipated microglial population obtained after Step 1 displayed a small, round cell body with few processes. In comparison, cells obtained after Step 2 displayed a similar-sized central soma but with multiple slender processes branching out to resemble a spider-web-like formation, anticipated to be OPCs. Cells attached to the flask after Step 2, proposed to be astrocytes, were then passaged into a T-75 flask to expand the cell line. Immunohistochemistry (IHC)-based validation of the separated microglial and OPC population was not performed due to bacterial contamination of the culture (**Figure 5**).

Figure 5: Microglia and OPCs separated from mixed glial culture to purify astrocytes. The s*upernatant containing superficially adhered microglial population after Step 1(S1) and loosely-adhered OPCs after Step 2(S2), respectively, was further cultured to validate cellular populations obtained. Astrocytes remaining in the culture after Step 2 were freshly plated in a pre-coated T-75 flask.*

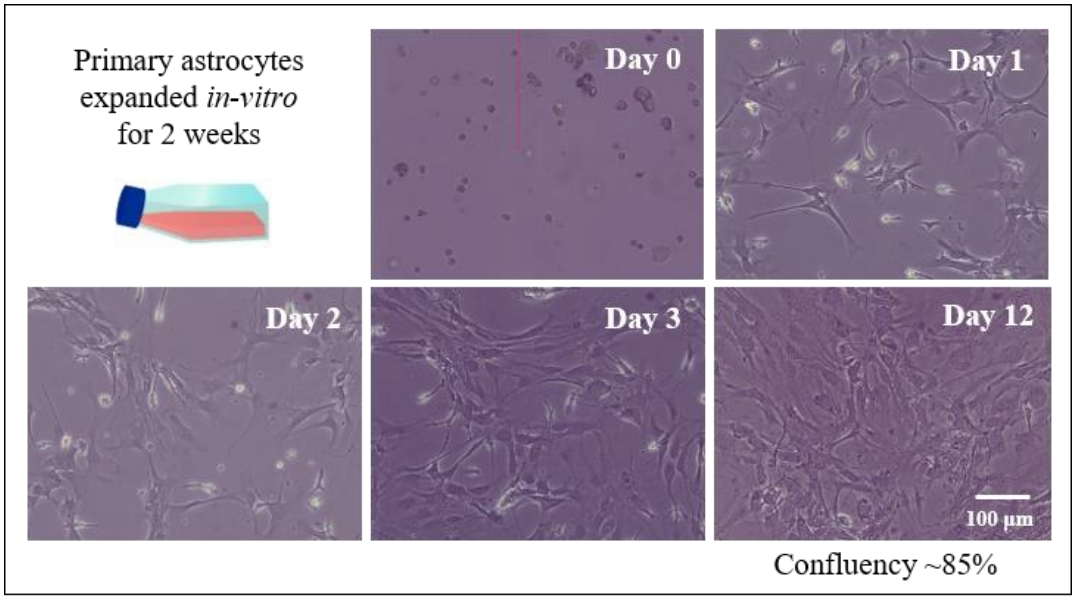

Figure 6: Primary mouse astrocytes expanded in vitro for 2 weeks. *Bright-field images showing a change in astrocyte morphology over-time, attaining around 85% confluency by Day 12.*

Purified astrocytes at Day 0 following passaging into a T-75 flask remain freely suspended in the culture media and display a spherical morphology (**Figure 6**). By Day 1, astrocytes demonstrate successful attachment to the PLL-coated growth surface and begin exhibiting characteristic astrocyte morphology, indicated by a central soma with multiple thin processes branching out. The observed increase in the confluency of the culture over time indicates the proliferation of astrocytes. To facilitate robust growth and healthy culture conditions, media was changed once in 2 days for freshly isolated primary astrocytes. By Day 3, astrocytes thus obtained, displayed much bigger cell bodies with multiple long processes emerging from the soma to form an interconnected meshwork of astrocyte-containing monolayer. By day 12, the culture system shows confluency of around 85%, approximated by visual estimation. (**Figure 6**).

2. Characterization of the astrocyte culture system

To validate the astrocyte purity in the culture, the cellular composition of the culture was characterized. Immunocytochemistry (ICC) labeling for cell-type-specific proteins was performed to identify the cell-types present in the culture (**Table 3**).

Protein markers	Cell-type identification
GLAST	Astrocytes (immature)
Olig1	Oligodendrocyte Precursor Cells (OPCs) and oligodendrocytes
NeuN	Mature neurons
Vimentin	Meningeal fibroblast
Iba1	Microglia
GFAP	Astrocytes (mature/reactive)

Table 3: *Cell-type-specific protein markers used to characterize the cellular identity*

Expression of the astrocyte-specific proteins, Glutamate/aspartate transporter (GLAST) and Glial Fibrillary Acid Protein (GFAP), was observed in morphologically-distinct astrocyte populations. Compared to the immature GLAST+ astrocytes, the mature GFAP+ astrocytes exhibit smaller cell bodies with long, thin extending processes (**Figure 7, B, C).** Astrocytes in culture have been proposed to inherently exhibit a reactive phenotype due to the artificial *in vitro* conditions, which is characterized by upregulated GFAP expression (Du et al., 2010). Astrocytes maintained in culture in the T-75 flask for a shorter duration predominantly label for GLAST, which is suggestive of a more immature phenotype (**Figure 7, B)**. In contrast, majority of the astrocytes maintained in culture for a prolonged period express the GFAP protein, possibly reflecting a more mature phenotype. However, a high number of GFAP+ cells in the culture may also suggest a gradual inheritance of a reactive phenotype of the astrocytes (**Figure 7, C).** With the expression of both the GLAST and GFAP proteins observed in glial precursors as well as mature cells (Shibata et al., 1997), discerning the exact maturation stage of the astrocytes in culture is not straightforward.

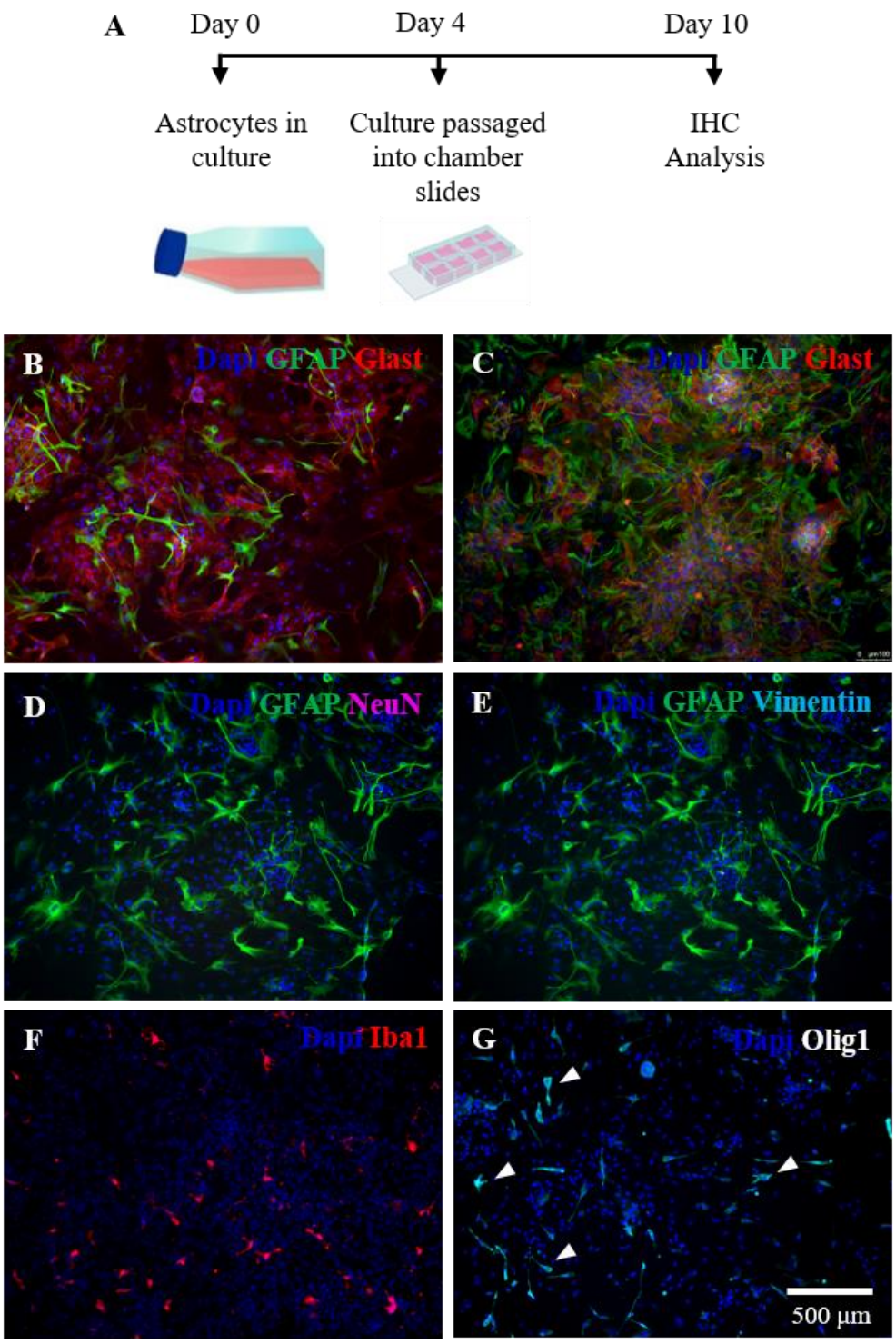

Figure 7: ICC analysis of cell culture reveals the presence of multiple cell types in the culture. *Cell-type-specific proteins GLAST to label immature astrocytes, GFAP-label mature and reactive astrocytes in culture* ***(B, C)*** *NeuN to label mature neuronal cells* ***(D)****, Vimentin to label meningeal fibroblasts* ***(E)*** *Olig1 to label OPCs (indicated by arrows)* ***(G)****. ICC counterstained with DAPI.*

Ionized calcium-binding adaptor molecule 1 (Iba1) protein was used as a marker to identify microglia in the cell culture (Korzhevskii & Kirik, 2016; Ohsawa, Imai, Sasaki, & Kohsaka, 2004). Iba+ microglia were observed in the culture, possessing characteristic morphology of central soma and extending processes smaller than the astrocyte processes (**Figure 7, F).** Oligodendrocyte transcription factor (Olig1) indicate the presence of OPCs and oligodendrocytes in the culture (Dai, Bercury, Ahrendsen, & Macklin, 2015; Schebesta & Serluca, 2009) (**Figure 7, G**), suggesting limited efficiency of the protocol to eliminate these cell types from the mixed glial culture. Importantly, the cells in culture do not label for Neuronal nuclear antigen (NeuN) or Vimentin, suggesting the absence of mature cortical neurons and meningeal fibroblasts respectively in the culture system (**Figure 7, D, E**).

3. In vitro Viral Transduction

To assess NeuroD1-mediated reprogramming *in vitro*, astrocytes in culture were transduced with AAV9-Control and AAV9-ND1-Reprogramming dual virus systems. To obtain maximum transduction efficiency, two Multiplicity of Infection (MOI) was chosen, a lower dose of 80,000, and a higher dose of 160,000, based on the MOI used by (AschauIer et al., 2013). Calculations for the AAV-9 viral titers are described in detail in **Appendix II**. AAV-9 viral solution was added to the cell culture media and incubated for 24 hours. 1-week post-transduction astrocytes were fixed and processed for ICC analysis.

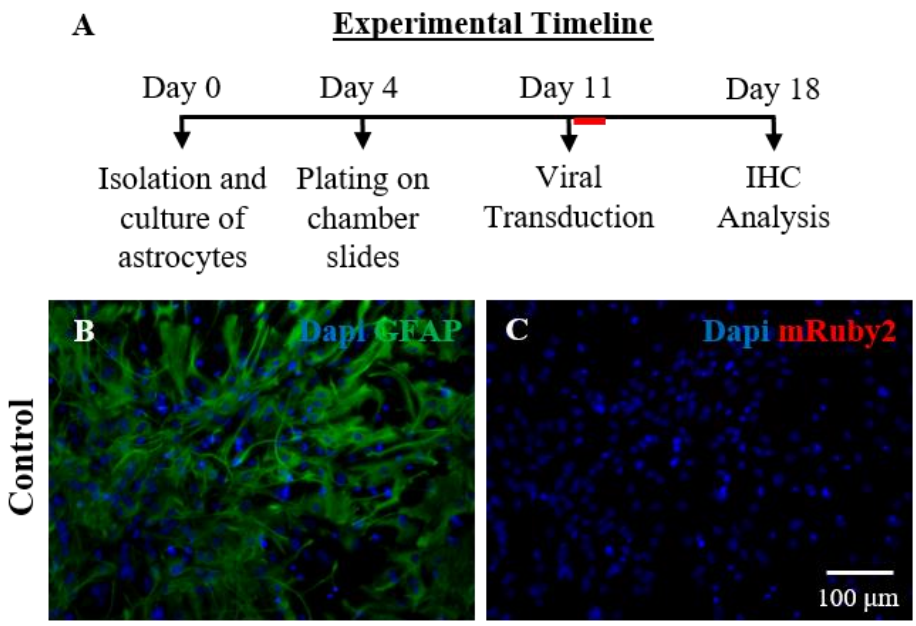

Figure 8: AAV-9 dual virus system at an MOI of 8*10^4 fails to transduce astrocytes in culture. *Astrocytes in a confluent culture were transduced with AAV9 at an MOI of 80,000.* ***(A)*** *Experimental timeline. Red bar indicating 24-hr viral transduction.* ***(B)*** *GFAP labeling astrocytes in culture.* ***(C)*** *Absence of mRuby2+ cells in culture.*

Viral transduction and expression in astrocytes, indicated by mRuby2 expression, was not detected at an MOI of 8*10^4 (**Figure 8, B, C**). While this MOI for AAV transduction has been shown to successfully transduce Neuro2A neuroblastoma cell line (Aschauer et al., 2013), it seems inefficient to transduce primary astrocytes in our system. This can indicate that the MOI of 8*10^4 may not be enough to achieve the co-transduction of mouse primary astrocytes simultaneously by two viral vectors.

By contrast, higher MOI of 1.6*10^5 was successful in achieving simultaneous transduction of both vectors, resulting in the expression of reporter mRuby2 and astrocyte to neuron reprogramming in the experimental condition, which will be discussed next (**Figure 9**).

In the Control condition, mRuby2 expression was observed in cells co-labeled with GFAP, indicating the transduction of astrocytes (**Figure 9, B-B''**). Unanticipatedly, IHC-labeling for Beta-III Tubulin (Tuj1), a marker for neural cells in early differentiation stages, detected the sporadic presence of Tuj1+ neurons in the Control transduced culture (**Figure 9, B''**). Transduction of the neurons, indicated by the mRuby2+/Tuj1+ neurons was observed to the same degree as astrocytes. This demonstrates the capacity of AAV-9

transduction of both astrocytes and neurons in culture. To note, in the mRuby2 control condition, the GFAP+ astrocyte populations maintained their highly inter-connected monolayer arrangement with limited cells expressing mRuby2+ (**Figure 9, B'**), indicating that the use of the virus did not cause any type of undesired effect.

By contrast, in the ND1-Reprogramming conditions, AAV9-transduced, mRuby2 expressing cells exhibited a global rearrangement to form multi-cellular clusters. These multi-cellular aggregations displayed a classical structure of a neuron-cell body with axonal projections connecting to cell clusters in the vicinity. The expression of reporter mRuby2 was limited to the aggregated cells in the center of the cluster. In contrast, GFAP+ astrocytes, in the absence of mRuby2 resembled the interconnected monolayer of astrocytes observed in the Control system (**Figure 9, C-C'**).

Further, a great number of Tuj1+ cells were enriched in the clustered cells, co-localizing with mRuby+ cells indicating potentially reprogrammed neurons. The enrichment of Tuj1+ cells in the multi-cellular cluster was much higher than the occasional Tuj1+ cells observed in the mRuby2-/GFAP+ astrocyte monolayer in the ND1- reprogramming condition (**Figure 10, B**). This indicates that the Tuj1+ neurons in the global cluster may be reprogrammed neurons. To note, a number of Tuj1+ cells in the cluster co-expressed GFAP, suggesting cells in the intermediate precursor stage, in the transition from astrocyte to neuron, as has been previously reported (Niu et al., 2013). A few GFAP+/Tuj1+/mRuby2+ clusters resembled neurosphere-like formation, where neural precursor cells aggregate to form a spherical structure (Jensen & Parmar, 2006; Zhou et al., 2016). The ends of extending processes emerging from these clusters possess the morphological characteristics of growth cones in axons of developing neurons (**Figure 10, B-B'**). However, as a caveat, there was the occasional presence of Tuj1+/mRuby2- neurons in the Control AAV-9 transduced culture system. This may indicate the presence of neural precursor cells in the cell culture that differentiated into Tuj1+ neurons and adds a layer of complexity to confirming the reprogramming.

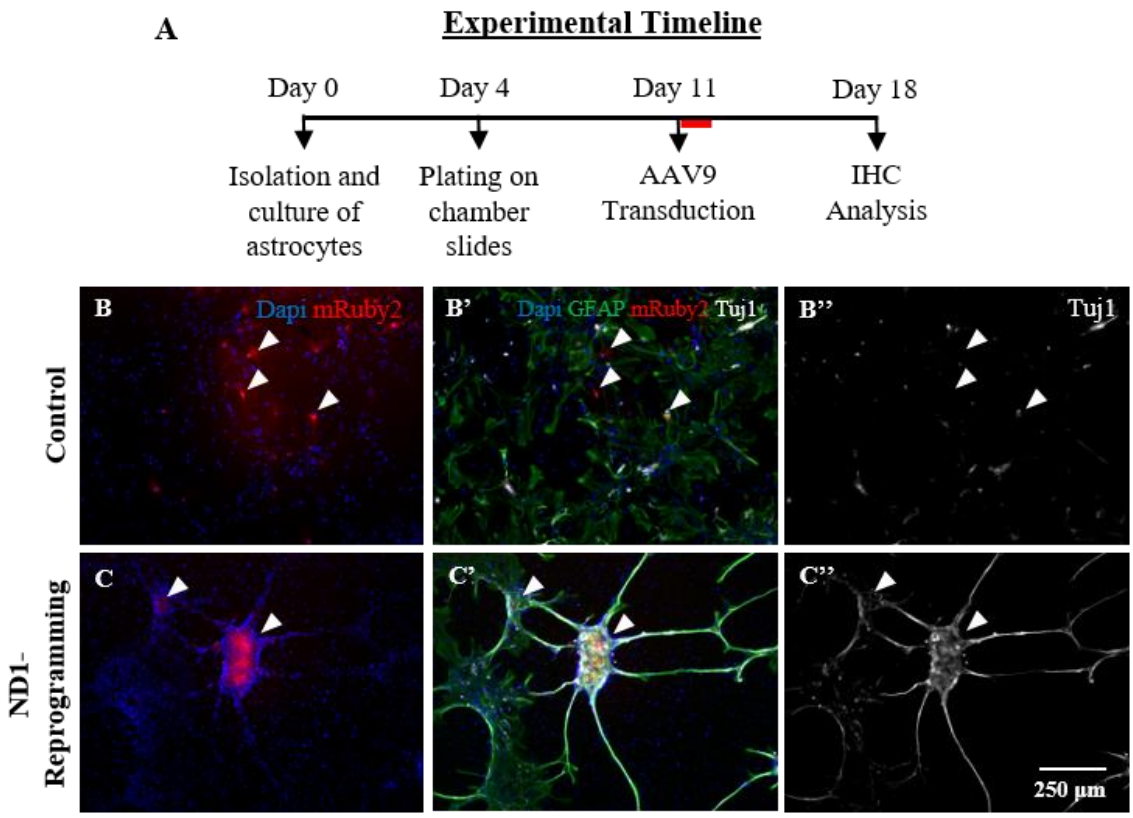

Figure 9: Expression of AAV-9 ND1-Reprogramming constructs reprograms astrocytes to neurons in culture. *Astrocytes in culture were transduced with a higher dose of MOI 1.6*10^5 and incubated for 24 hours.* ***(A)*** *Experimental Timeline. mRuby2+ cells indicating successful transduction in Control* ***(B-B'')*** *and ND1-Reprogramming condition* ***(C-C'').*** *mRuby2+ cells in the clusters in the ND1-reproramming conditions co-label for GFAP and Tuj1* ***(C').***

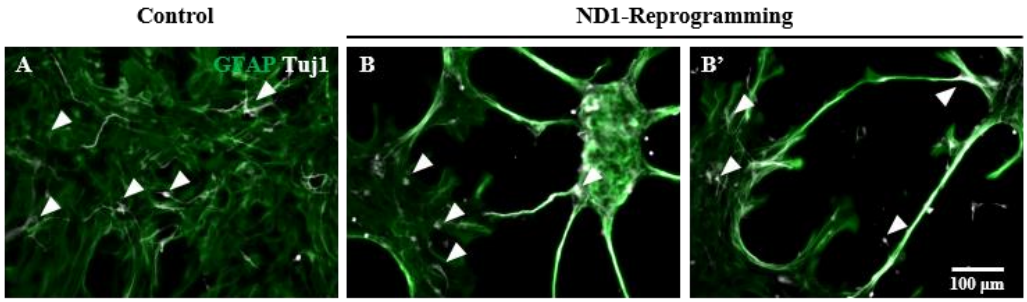

Figure 10: Reprogrammed astrocytes exhibit distinct morphological clustering compared to the Control condition. ***(A)*** *shows the presence of GFAP+ and Tuj1+ (indicated by arrows) cells in the culture 1-week post-transduction in the Control condition.* ***(B-B')*** *shows the distinct global clustered morphology in the ND1-Reprogramming condition. Arrows identify Tuj1+ cells in the ND1-Reprogramming condition.*

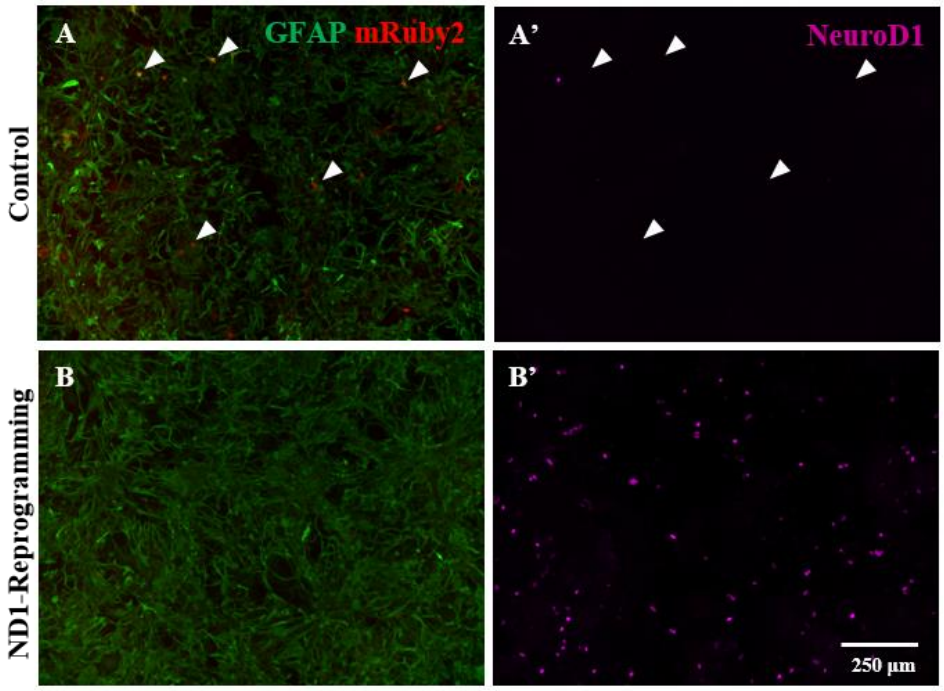

Figure 11: IHC analysis detects the expression of NeuroD1 in the ND1-Reprogramming condition. (A-A') *The control system shows expression of mRuby2 (indicated by arrows) but no NeuroD1 expression.* ***(B-B')*** *NeuroD1 expression observed in the absence of reporter mRuby2 in the ND1-Reprogramming condition.*

The successful expression of NeuroD1 was validated by IHC in the ND1-reprogramming system, indicating the functionality of the dual virus system (**Figure 11**). Together, the *in vitro* results demonstrate a successful expression of the two-virus system at a higher MOI of $1.6*10^5$. Enrichment of Tuj1+/mRuby2+ neuronal cells indicates a successful alteration of fate, suggesting the capability of the *in vitro* system as a model for interrogating NeuroD1-mediated neuronal reprogramming.

Taken together, the *in vitro* reprogramming model was successfully used to interrogate ND1-driven astrocyte to neuron reprogramming. The successful expression of the AAV-9 Control and ND1-Reprogramming system was validated. Astrocyte monolayer in the ND1-reprogramming condition showed a global rearrangement to form a clustered aggregation. mRuby2+ cells in the cluster co-label for astrocyte GFAP and neuronal Tuj1 protein marker, suggesting reprogramming. However, the efficiency of reprogramming observed was limited. Grande et al. (2013) demonstrated the influencing effects of the *in vivo* system to enhance reprogramming. This guided the next project goals-to assess the potency of NeuroD1-mediated reprogramming in the *in vivo* system.

SECTION 2 – *In vivo* Reprogramming

1. In vivo Viral Transduction

To test the potency of NeuroD1 to guide neuronal reprogramming *in vivo*, the AAV-9 dual virus system for the Control and ND1-reprogramming system was intracranially injected, targeted at the striatum of adult mice. First, the effect of the perturbation was evaluated. Injury to the brain has been demonstrated to elicit an inflammatory response, accompanied by the migration of astrocytes to the perturbed tissue region. Characterized by upregulated GFAP protein expression, these astrocytes are described to be in a 'reactive' state (Yu, Wang, Katagiri, & Geller, 2012). Immunohistochemistry for GFAP protein revealed the presence of GFAP+ reactive astrocyte around the injection stab site 1 week after intracranial injection (**Figure 12, A**). The GFAP+ cells were localized to the tissue regions around the injection stab site in the cortex and striatum (**Figure 12, B, C**), but were absent in the distal regions from the injection site and in the contralateral hemisphere of the brain, suggesting their reactive phenotype as a consequence of the stab wound. The abundance of reactive astrocytes around the injury region would serve as an advantage with a higher pool of cells available for reprogramming, as has previously been suggested (Guo et al., 2014).

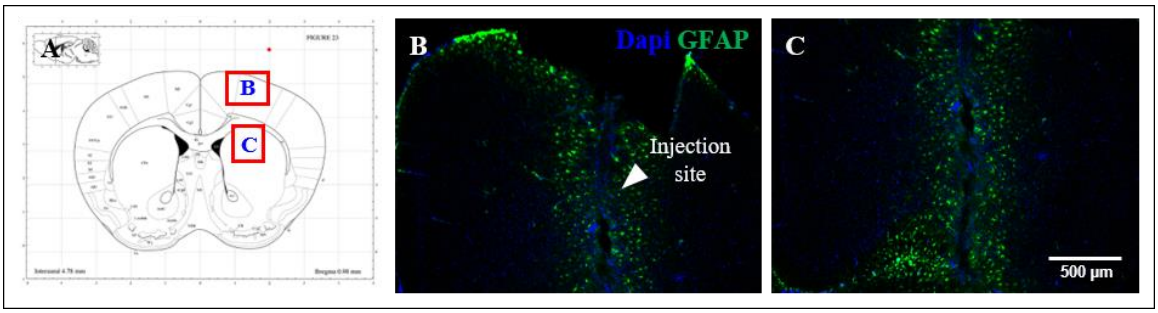

Figure 12: Reactive astrocytes induced at the injection site. *Reactive astrocytes, identified by the upregulated expression of GFAP protein, are observed in abundance along with the injection stab site (indicated by arrow) at the* ***(B)*** *Cortex,* ***(C)*** *Striatum.*

Next, to test reprogramming *in vivo*, intracranial injections of the Control and ND1-reprogramming system was performed. As described in the methods, a two-virus system was used for the Control and ND1-reprogramming condition. In both, the reporter mRuby2 was expressed in astrocytes co-transduced with the two vector system, the first- an AAV9-GFAP::Cre driver construct and the second-the reporter mRuby2 construct. The viral titers

for the intracranial injections are shown in **Table 4**. IHC was performed on isolated brain sections 1-week after viral transduction to assess reprogramming.

		AAV	Titer GC/µl
	Exp	AAV9-CAG-DIO-NeuroD1-P2A-mRuby2	1.82E+11
Con		AAV9-GFAP-Cre	1.67E+11
		AAV9-CAG-DIO-mRuby2	3.15E+11

Table 4: *Viral titer for each construct used for the intra-cranial injection in Control (Con) and ND1-Reprogramming (Exp)*

To note, analysis of the Control-mRuby2 transduced condition produced surprising results and shifted the direction of the project goals, thus the following results describe the observation in the Control-mRuby2 injected brains only. Although the injection was targeted at the striatum, expression of mRuby2 was often observed in the cortex surrounding the stab site. Leak and diffusion of viral solution through the injection site was speculated to produce this observation. As designed, expression of the reporter mRuby2 was observed in astrocytes co-labeled with GFAP and exhibit characteristic astrocyte morphology with central cell body and emerging processes (**Figure 13, A-A'**). However, mRuby2+/GFAP co-labeled astrocytes were observed in a surprisingly low abundance.

In contrast, expression of the reporter mRuby2 was observed in large groups of mature resident neurons in the cortex (**Figure 13, B**). Specifically, the mRuby2+ neurons exhibited a large pyramidal-shaped cell body with a single linear axonal projection extending towards the outer cortical regions. The arrangement of the mRuby2+ cells resembled the spatial arrangement of mature functional neurons in the cortical layers of the endogenous circuitry (**Figure 13, B-B'**). This unanticipated result in the Control dual virus system was evidence that may indicate the transduction and expression of the AAV9 virus in the resident neurons.

Collectively, mRuby2 expression is seen predominantly in neurons as compared to astrocytes, suggesting (1) an inherent tropism of AAV-9 to preferentially transduce neurons or (2) the restricted ability of astrocytes to be transduced. While the AAV9 tropism towards neuronal cells has been well-characterized (Aschauer et al., 2013; Zincarelli et al.,

2008), the activity of GFAP promoter in mature neurons, although reported earlier, has not received much attention (Hol et al., 2003; Y. Lee, Messing, Su, & Brenner, 2008).

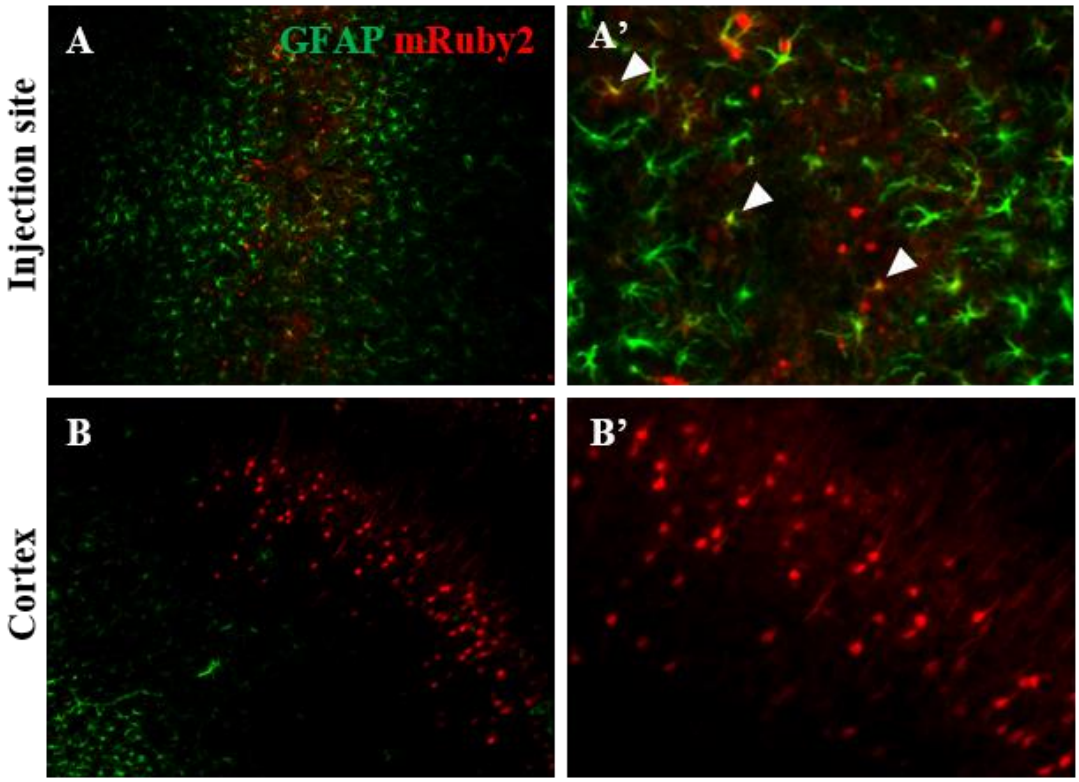

Figure 13: Reporter mRuby2 expression observed in astrocytes and neurons in the Control Dual-virus system in vivo. (A-A') *mRuby2+ cells present along the injection site at the striatum. Arrows showing mRuby2+ cells co-localizing with astrocyte marker GFAP.* ***(B)*** *mRuby2+ cells in the cortex. Enlarged view in* ***(B').***

Following this observation, the research goals were redirected to interrogate the expression pattern of the GFAP::Cre construct in order to better understand the transduction capacity of the viral system.

2. Characterizing AAV9-GFAP::Cre transduction and expression

To characterize the cellular expression pattern of AAV9-GFAP::Cre, the viral construct was delivered intracranially in a reporter Ai9-tdT mouse (**Figure 14, A**). Expression of reporter tdTomato is obtained only in the presence of Cre recombinase, in this case, driven by the GFAP promoter, widely established to be specific to astrocytes (Andræ et al., 2001; Griffin et al., 2019). Ai9-tdT mice, aged >8weeks were intracranially injected with 3 µl of AAV9-GFAP::Cre virus-containing $1.6*10^{11}$ VG content. Whole-brain was isolated 1-week post-injection and processed for IHC (**Figure 14, B**).

Corroborating previous observations, as described in **Figure 13**, transduction and expression of the GFAP::Cre construct was observed along the site of injection at the cortex and striatum, indicated by the expression of reporter tdTomato (**Figure 14, C, D-D'**). IHC analysis of the cortex revealed some tdT+ cells co-labeled with GFAP, possessing astrocyte-like morphology (**Figure 14, E**). However, following a similar pattern observed previously, the majority of tdT+ cells co-expressed the neuronal marker NeuN (**Figure 14, E'**). Preliminary quantification of the tdT+ cell types from three technical replicates shows preferential transduction and expression of viral constructs in NeuN+ neuronal cells (**Figure 15, B)**. Taken together, this corroborates previous observations and provides further evidence to the transduction and expression of AAV9-GFAP::Cre construct in both astrocytes and neurons in the cortex.

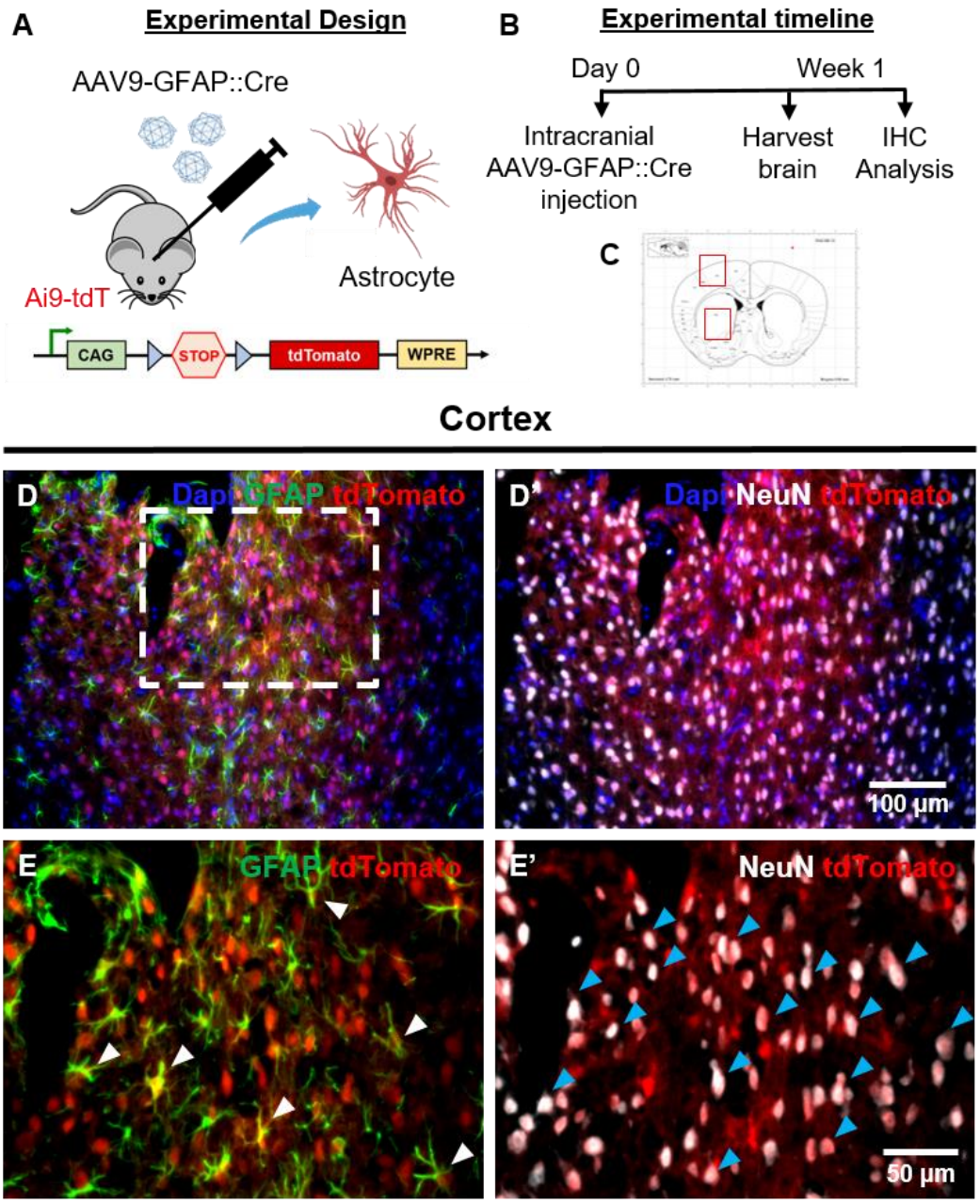

Figure 14: Intracranially delivered AAV9-GFAP::Cre expressed in astrocytes and neurons. (A) *Schematic representation of the experimental design. Astrocytes transduced by the AAV9-GFAP::Cre viral system express reporter tdT, that is driven by the viral GFAP promoter.* ***(B)*** *Experimental timeline.* ***(C)*** *Red boxes outline the injection site at the cortex and striatum.* ***(D-D')*** *Expression of endogenous reporter tdT around the injection stab site at the cortex.* ***(E-E')*** *Enlarged view of the white box.* ***(E)*** *Arrows indicating tdT+ cells with astrocyte morphology and co-label with GFAP.* ***(E')*** *Blue arrows indicating tdT+ cells co-labeled with NeuN, possessing neuronal morphology.*

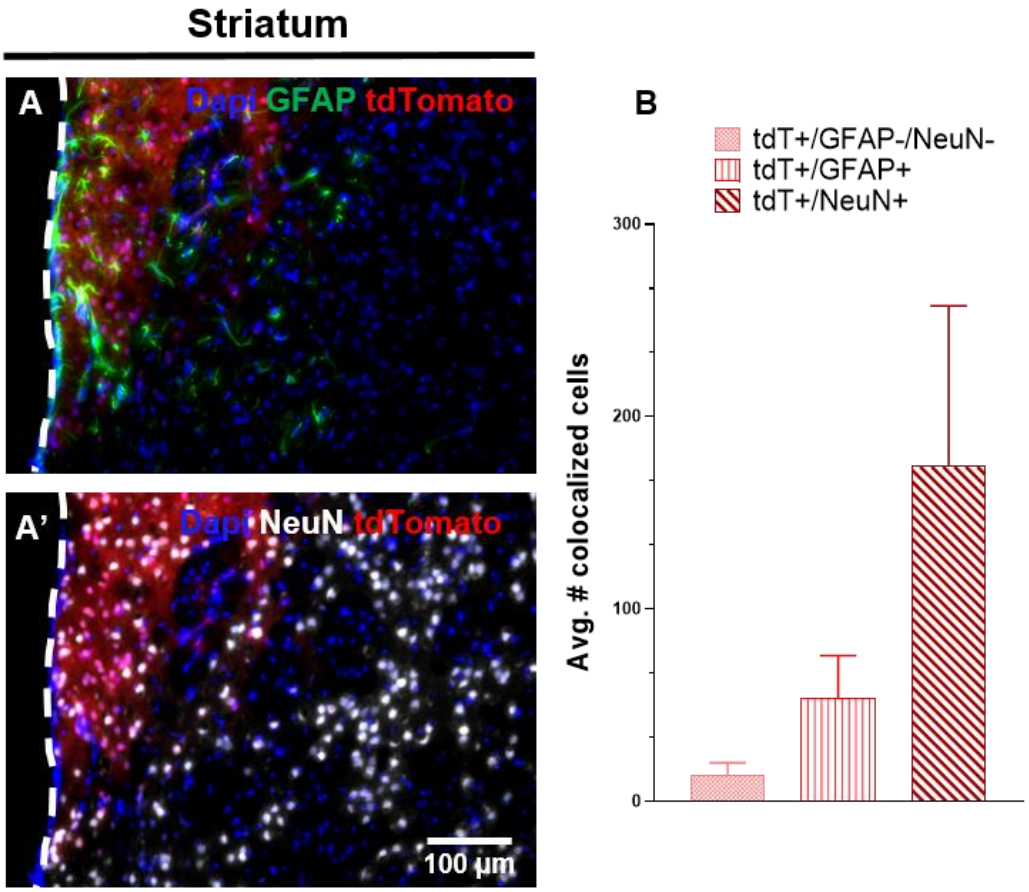

Figure 15: Intracranially delivered AAV9-GFAP::Cre expressed in astrocytes and neurons in the striatum. (A-A') *distinct populations of tdT+ cells co-label with astrocyte marker GFAP and neuronal marker NeuN, indicating transduction of both cell-types. The white dotted line indicates the lining of the lateral ventricles.* ***(B)*** *Quantification of cell-type transduction in cortex using ImageJ (n=3 technical replicates - 3 brain section from one mouse brain).*

The AAV9-GFAP::Cre expression pattern observed in the cortical astrocytes and neurons was replicated in the striatum (**Figure 15, A-A').** Despite the viral injection targeted to the caudate-putamen regions of the striatum, in the initial analyses, tdT+ cells were observed in the regions lining the lateral ventricles and absent from the striatal parenchyma. This could indicate potential viral diffusion into the ventricles, thus, transducing cells only in the vicinity. Modified injection sites targeting deep into the striatum were subsequently chosen to ensure successful delivery into the striatum, which thus, limited its diffusion to adjacent tissue regions. Collectively, of the transduced cells observed, qualitative IHC analyses revealed limited expression of the reporter tdT in GFAP+ astrocytes, but predominantly in neurons.

Collectively, the results reveal intriguing expression patterns of the viral GFAP-promoter delivered using the AAV9 system. In particular, all tdT+ astrocytes co-label with GFAP expression that is indicative of a reactive astrocyte phenotype. This suggests the biological features of reactive astrocytes that facilitate easy uptake and express of viral constructs. More importantly, expression of GFAP::Cre in neurons poses intriguing questions. (1) Does AAV-9 possess a preferential cellular tropism towards neurons? (2) Is the tdT expression faithfully regulated by the Cre recombinase? And if so, (3) Do neurons in perturbed conditions upregulate GFAP promoter activity that facilitates better transduction and expression of viral vectors? To answer these questions, a different experimental approach was devised. Intravenous delivery of the AAV9-GFAP::Cre virus was performed to model a non-injury system, thus, enable the understanding of the system in the absence of CNS perturbation.

3. Intravenous delivery of AAV9 viral vectors

Intravenous delivery of AAV-9 was performed to address two specific goals. First, to characterize the efficiency of AAV-9 in transducing cells of the brain when delivered systemically. Compared to other viral vectors, AAV9 has the unique ability to cross the blood-brain-barrier (BBB), an attribute that has made it a potential non-invasive gene delivery vector for gene therapy. Combined with its minimal off-target effects, the AAV9 gene platform has been successfully approved for clinical use in humans (Lykken et al., 2018). Second, to characterize the cell-type tropism of intravenously delivered AAV-9 compared to the intracranial delivery mode. Foust et al. (2009) demonstrated intracranially delivered AAV-9 to preferentially transduce neurons while intravenous delivery resulted in preferential transduction of astrocytes in the brain. Thus, intravenous delivery of AAV9-GFAP::Cre was performed next, in order to assess the efficiency of this approach to enhance transduction expression of ND1 specifically in astrocytes.

Following the methodologies described by Foust et al. (2009), AAV9-GFAP::Cre virus was injected through the tail-vein in an Ai9-tdT mouse aged 7-8 weeks (**Figure 16, A, B**). 3µl of virus solution in sterile saline with $4.5*10^{11}$ GC was injected through the tail vein. Nicole Emmitt, a graduate student in the Low lab, performed the tail vein injection.

2 weeks post-injection, mice were sacrificed and whole-brain isolated for IHC analysis (**Figure 16, B**).

Intravenous delivery of AAV-9 resulted in limited expression of reporter tdT in the cortical and striatal cells (**Figure 16, C**), scattered across estimated 2.8mm of the brain tissue on the rostrocaudal axis; this result was less robust than would be predicted based on the previous literature (Foust et al., 2009; Zhang et al., 2011). However, as anticipated, systemic AAV-9 delivery resulted in cellular transduction in both hemispheres, albeit in a limited fashion. The percentage of AAV9 particles successfully crossing the BBB can provide an explanation for this observation. To identify the cellular tropism of AAV-9 in the CNS, IHC was performed with the astrocyte marker GFAP and neuronal marker NeuN. The expression of mRuby2 was observed in cells with astrocyte-like bushy morphology (**Figure 16, D-D'**). However, validation of GFAP::Cre expression in astrocytes could not be confirmed due to the lack of GFAP labeling of astrocytes. As observed in previous experiments, tdT expression was again observed in mature neuronal cells. tdT+ cells exhibiting neuronal morphology were co-labeled for NeuN, confirming the cellular target (**Figure 16, E-E'**).

Taken together, the AAV-9 intravenous delivery strategy demonstrates limited efficiency to target the striatal and cortical cells in the CNS. There was no observed bias in cellular transduction between the cortex and the striatum, and no preferential targeting of astrocytes as opposed to neurons with intravenous viral delivery. The GFAP::Cre expression in mature neuronal cells was recapitulated in the systemic delivery model. IHC analysis for the expression of Cre recombinase protein will be crucial to confirm the successful targeting of AAV9-GFAP::Cre in the tdT+ cells.

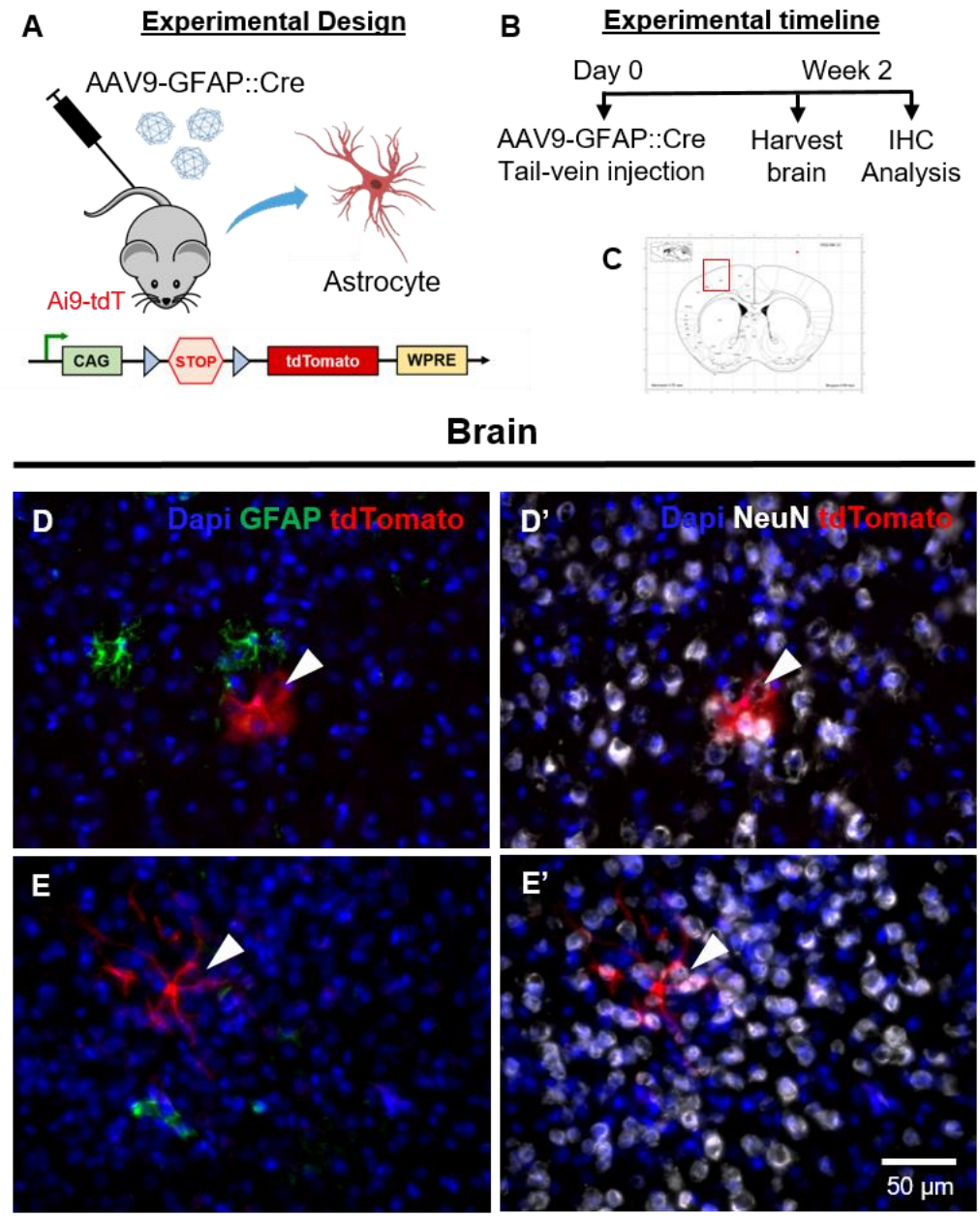

Figure 16: Intravenously delivered AAV9-GFAP::Cre demonstrates limited transduction efficiency in the brain. ***(A)*** *Schematic representation of the experimental design. Astrocytes transduced by the AAV9-GFAP::Cre viral system express reporter tdT, that is driven by the viral GFAP promoter.* ***(B)*** *Experimental timeline* ***(C)*** *Red box outlines tissue regions with reporter tdT-expressing cells.* ***(D-D')*** *tdT+ cell (indicated by arrow) shows astrocyte-like morphology with central soma and bushy peripheral processes and does not co-label for neuronal marker NeuN.* ***(E-E')*** *tdT+ cell displaying characteristic neuronal morphology with long slender axons-like structures and co-labels with NeuN (indicated by arrow). IHC counterstained with DAPI.*

A major concern of systemically administered gene-therapy using a viral gene delivery platform is its potential off-target effects on the peripheral system. To assess the potential

non-specific expression of the AAV9-GFAP::Cre system, expression of the reporter tdT in peripheral organs was characterized.

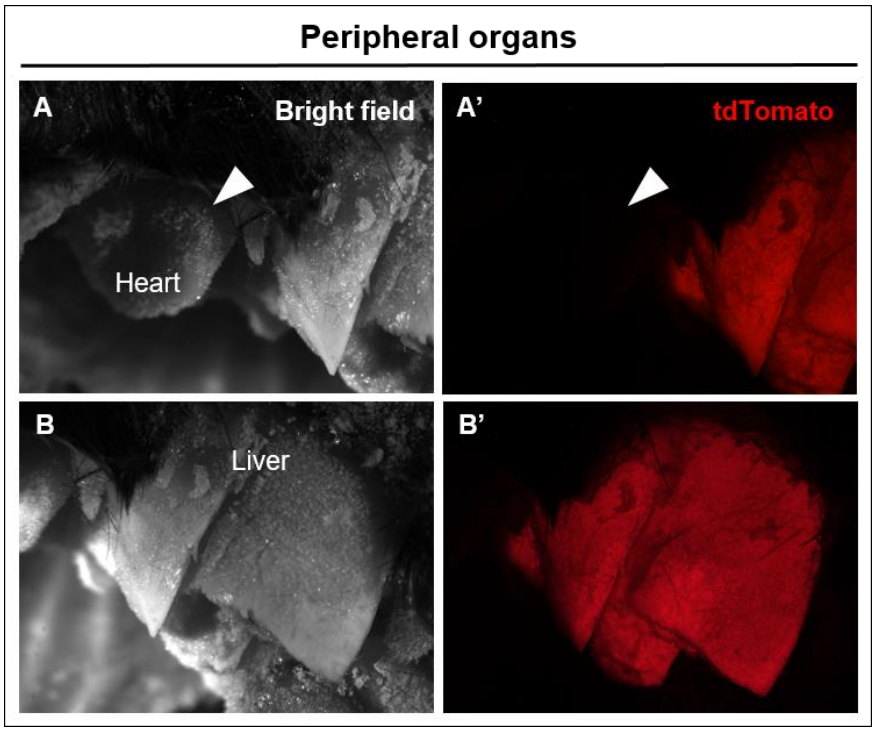

Figure 17: Intravenous delivery of GFAP::Cre is expressed in the liver. *Reporter tdT expression indicates GFAP promoter activity in transduced cells of the liver. Arrow indicates the absence of reporter tdT in the heart but exclusively limited to the liver tissue.*

Expression of the reporter tdTomato was observed in the liver and appeared to be limited exclusively to the liver amongst the peripheral organs (**Figure 17, A-A'**). Intravenously delivered AAV9 has been demonstrated to exhibit tropism for multiple peripheral tissue types such as the liver, heart, and muscle (Schuster et al., 2014; Zincarelli et al., 2008). While AAV9 transduction in the peripheral tissue was anticipated, specific expression of the GFAP::Cre construct in the mature hepatic cells was an intriguing result. This suggests the potential activation of the plasmid GFAP promoter in hepatic cells, highlighting the nuances of employing a GFAP promoter for gene therapy. Assessing the expression of Cre recombinase in the hepatic tissue would be important to determine the stringency of tdT expression.

Together, using contrasting gene delivery approaches facilitated the identification of unanticipated features of the designed viral constructs. However, GFAP::Cre expression

in both the systems share some common features: (1) GFAP promoter activity is observed in astrocytes, and, surprisingly, in neurons as well. Owing to the successful higher transduction efficiency obtained through the intracranial AAV-9 delivery, this method was chosen for future reprogramming experiments.

4. In vivo reprogramming in 6-OHDA Parkinson's disease mouse model

The ultimate aim of the project is to reprogram striatal astrocytes to neurons in the context of Parkinson's disease (PD). To assess the functionality of the AAV-9 dual virus system to drive forced expression of ND1 in a PD model, a well-established chemically-induced 6-OHDA PD murine model was used.

The PD model was established following methodologies from a previously published paper by Rivetti Di Val Cervo and colleagues (Rivetti Di Val Cervo et al., 2017). 6-OHDA was intracranially injected to target the dopaminergic projections of the nigrostriatal pathway in the Medial Forebrain Bundle (MFB). 10 days following the 6-OHDA injection, Control or Reprogramming dual virus system was delivered to the striatum by unilateral intracranial injection. 1-week post-injection of the virus, mice were sacrificed and whole brain tissue isolated for analysis (**Figure 18, A**).

As anticipated in any injured brain, GFAP-upregulated reactive astrocytes were observed in abundance in the ipsilateral hemisphere. In contrast to the presence of reactive astrocytes limited to the injection stab site in the previous experiments, the 6-OHDA injected brains exhibited an enrichment of reactive astrocytes throughout the striatal parenchyma as well as around the cortical injection stab site. GFAP+ astrocytes were absent in the contralateral hemisphere serving as an internal control, thus, confirming the limited regional effect of the perturbation. The widespread presence of GFAP+ reactive astrocytes may suggest a combinatorial effect of the neurotoxin as well as the injection stab in the ipsilateral striatum (**Figure 18, B**). To examine the effect of the neurotoxin on striatal dopaminergic neurons, IHC for DARPP-32, a dopamine-regulated neuronal phosphoprotein (which is specific to the striatum), was performed. However, no specific DARPP32 expression was observed, thus, precluding any comprehensive analysis. Future experiments would be directed at targeting a variety of dopaminergic markers to validate the neurotoxic effects of 6-OHDA.

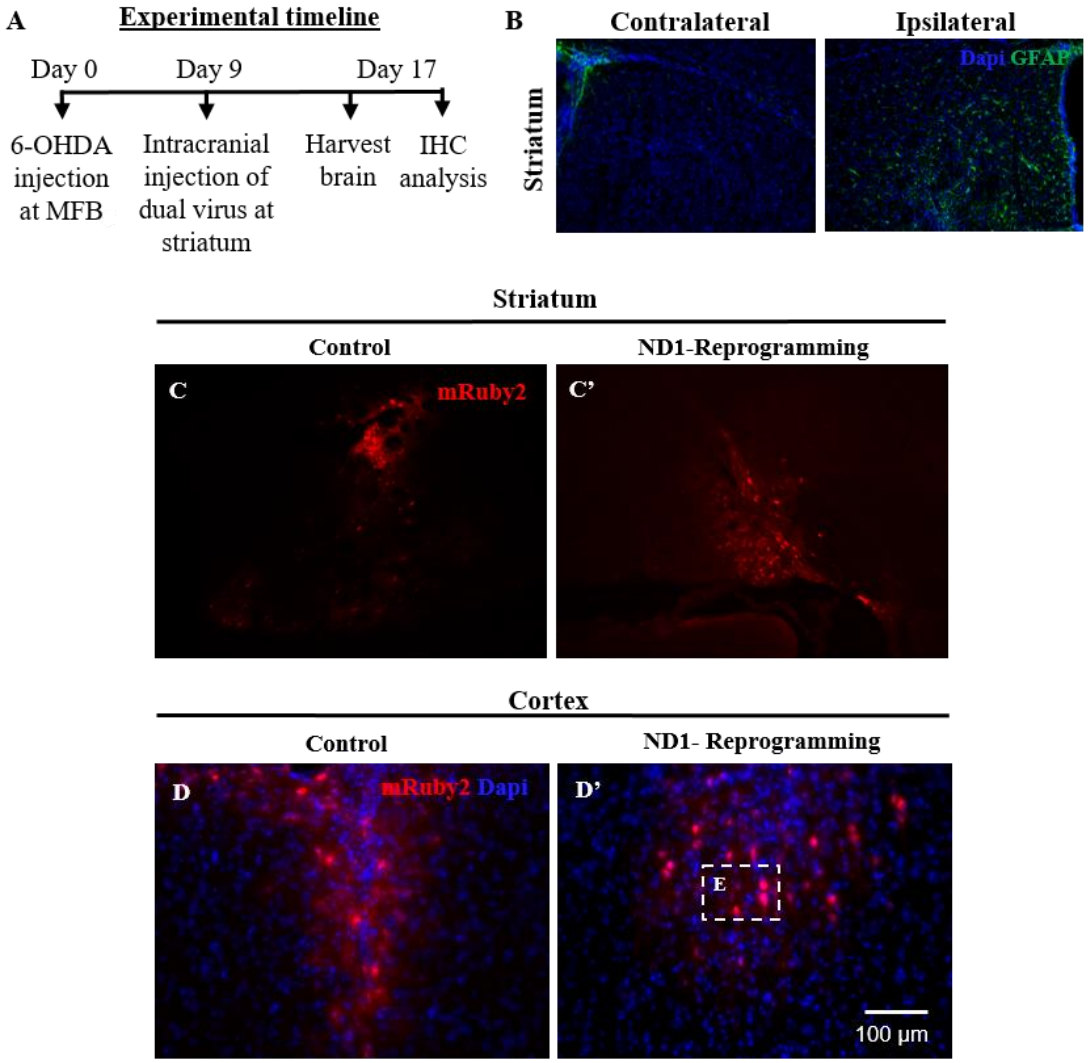

Figure 18: In vivo ND1-mediated reprogramming in a Parkinson's disease mouse model. (A) *Experimental timeline* ***(B)*** *Presence of GFAP-upregulated reactive astrocytes observed in the ipsilateral striatum and absent in the contralateral hemisphere.* ***(C-C)*** *mRuby2 indicates limited transduction in the ipsilateral striatum in both Control and ND1-reprogramming conditions.* ***(D-D')*** *mRuby2+ cells observed around the injection stab site in the cortex. While the majority of the mRuby2+ cells in the Control display astrocyte like-morphology, mRuby2+ cells in the ND1-condition display neuron-like morphology.*

Next, the efficiency of AAV-9 cellular targeting, indicated by mRuby2+ expression in the 6-OHDA model was examined. In both Control and ND1-reprogramming conditions, the presence of mRuby2+ cells was observed exclusively in the ipsilateral hemisphere of injection, confirming limited diffusion of viral particles. Paralleling the results observed in the previous experiments, mRuby2+ cells in the striatum were fewer in number and restricted to the tissue surrounding the ventricles (**Figure 18, C-C'**). This suggests two possibilities: (1) the limited efficiency of the AAV serotype 9 to target striatal cells, or (2) biological environment of the striatum conferring resistance to uptake virus. While the regional transduction patterns were consistent with previous observations, preliminary characterization of the mRuby+ cell-types in the cortex produced intriguing results (**Figure 18, D-D'**).

In the Control system, mRuby2+ expression was predominantly observed in cortical astrocytes, identified by the morphology and co-label with GFAP (**Figure 19, A-A'**). By contrast, in the ND1-reprogramming system, mRuby2+ cells exhibit neuronal morphology (**Figure 19, B-B'**). Further examination of the mRuby2+ neuronal-like cells in the cortex revealed two distinct populations, based on NeuN expression. As observed previously in **Figure 13**, **Figure 14**, one population of the mRuby2+ cells co-labeled with NeuN, indicating the expression of the AAV-9 constructs in the mature resident neurons. Intriguingly, another population of mRuby2+ cells failed to co-label with NeuN but possessed neuron-like morphology with a large cell body and a single extending process (**Figure 19, C'-C''**). This may indicate the potentially newly reprogrammed neurons that are in the early stages of maturation, hence fail to express the mature neuron marker, NeuN. The intensity of mRuby2 in the mRuby2+/NeuN- cells appear to be higher than the mRuby2+/NeuN+ neurons, possibly due to the robust expression of the ND1-mRuby2 reporter construct. The proposed reprogrammed neurons display morphological irregularities compared to the NeuN+ resident neurons. Labeled by the reporter, these cells display multiple tiny extending processes from the soma that is not characteristic of resident cortical neurons (**Figure 19, C'-C''**). This could be indicative of the reprogrammed neurons in a transition phase, where astrocytic processes are withdrawn and instead,

developing neurites emerge from the soma guided by extrinsic environmental cues. Going further, IHC validation of NeuroD1 expression will be required to validate the reprogramming.

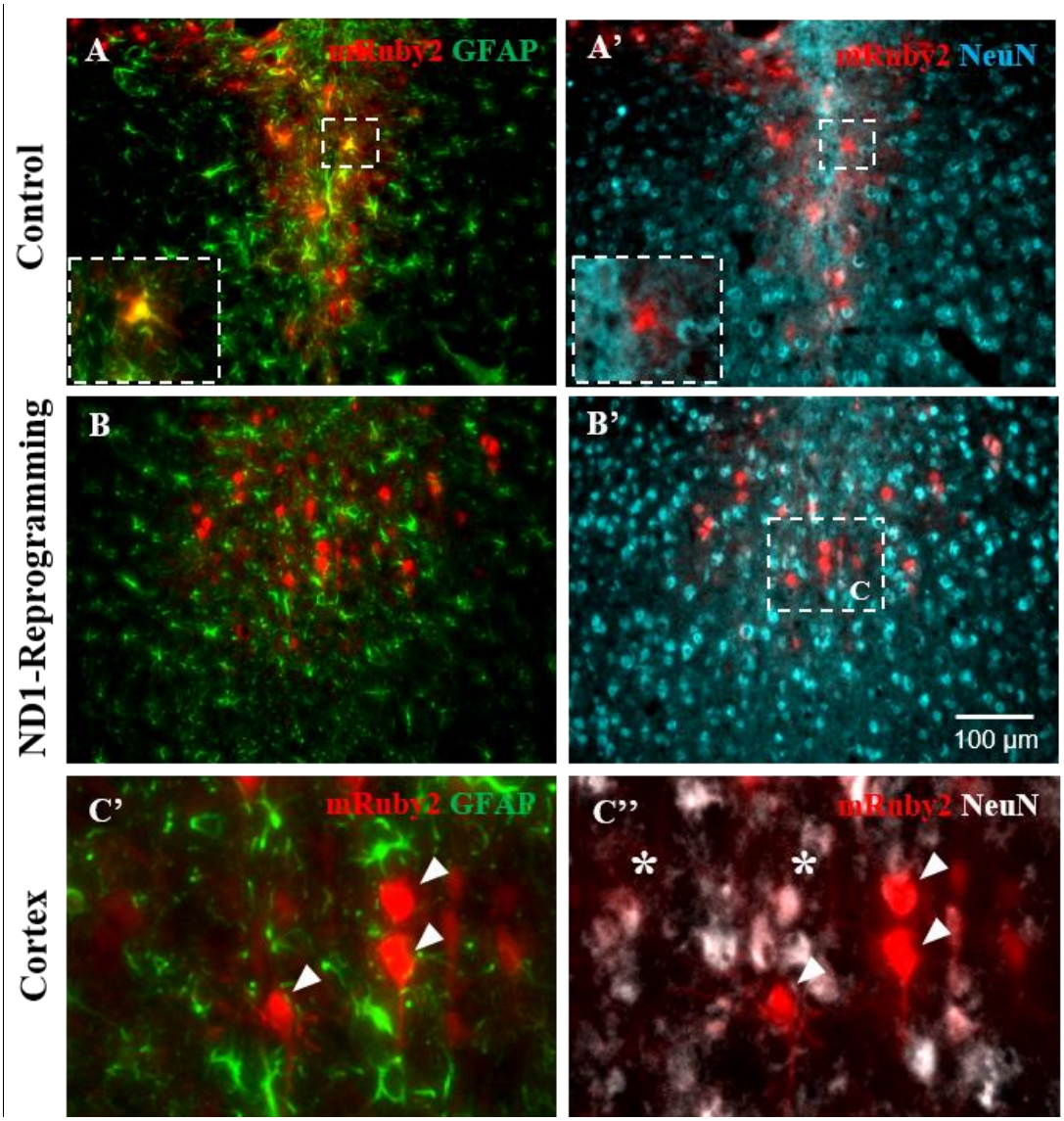

Figure 19: IHC analysis of the ND1-dual virus injected in the 6-OHDA mouse model. (A-A') *mRuby2+ astrocytes co-label with GFAP in the Control condition (inset).* ***(B-B')*** *most of the mRuby2+ cells display neuronal morphology and do not co-label with GFAP in the ND1-reprogramming condition.* ***(C-C')*** *Enlarged view of the white box C. Two distinct populations of neuronal mRuby2+ cells observed in the ND1-Reprogramming condition, one colocalizing with NeuN (indicated by an asterisk), and the other does not co-label with NeuN (indicated by arrows).*

Overall, the contrasting results obtained from the *in vitro* and *in vivo* systems provide different perspectives on NeuroD1-mediated reprogramming. The following broad conclusions can be made taking together all the evidence presented here:

1. The expression of the AAV-9 Control and ND1-Reprogramming dual virus system was successfully validated in the *in vitro* culture system. Global rearrangement of AAV-9-ND1 transduced astrocytes, along with co-expression of astrocyte and neuronal proteins, could indicate the potential transition of astrocytes to an immature neuronal precursor stage, induced by ND1-mediated reprogramming.

2. AAV-9-GFAP::Cre shows the ability to target mature, resident neurons in the cortical layers in both the intracranial and intravenous delivery models, highlighting the neuronal tropism of the AAV-9 system and the activity of GFAP promoter in neurons. This warrants careful design and interpretation for any future *in vivo* AAV-9 GFAP::Cre based astrocyte to neuron reprogramming system

3. The expression of the AAV-9 Control and ND1-Reprogramming dual virus system was successfully validated in the 6-OHDA Parkinson's disease (PD) model. Combinatorial targeting of the AAV-9 viral construct was observed in the mature resident neurons as well as potentially reprogrammed neurons in the cortex.

CHAPTER IV: DISCUSSION

The current study aims to develop an Adeno-Associated Virus-based approach to NeuroD1-mediated direct neuronal reprogramming in a Parkinson-disease mouse model. First, the successful expression of the AAV-9 gene delivery system was validated using an *in vitro* system. AAV9-mediated forced expression of NeuroD1 (ND1) in astrocytes was observed to induce a fate conversion by transitioning through an immature precursor stage. Having validated this, the ability of ND1 to drive astrocyte conversion to neurons *in vivo* was assessed. Characterization of the AAV9-GFAP::Cre viral construct expression revealed the unanticipated activity of the astrocyte GFAP promoter in mature resident neurons. This effect was consistently observed using both intracranial and intravenous gene delivery approaches. Finally, to examine the ability of ND1 to drive reprogramming in the context of neurodegenerative diseases, a chemically-induced 6-OHDA Parkinson's disease model was used and the expression of the AAV9-ND1 viral construct was observed in mature resident neurons as well as potentially reprogrammed neurons. Thus, this study demonstrates a novel, combinatorial approach to neuronal regeneration using the proneural transcription factor ND1. First, the use of GFAP promoter driven ND1 to reprogram supporting astroglia to neurons. Second, this study proposes the use of AAV9 GFAP::Cre to target directly to resident neurons, which can be leveraged for gene therapy to enhance neuronal survival in the context of brain injury and neurodegenerative diseases such as Parkinson's disease and Alzheimer's disease.

The multi-cellular neuron-like global rearrangement of the astrocytes in the ND1 conditions *in vitro* pose interesting questions. Astrocytes in the monolayer, transduced with the AAV-9 reprogramming constructs seem to aggregate to form clustered arrangements. These clusters extend multiple processes to connect to adjacent cell clusters. A few clusters resembled the spherical, high cellular density aggregations termed as neurosphere. The free-floating neurospheres are composed of neural stem cells (NSCs) and offer a simple model to gain insight into the molecular and cellular functions of NSCs *in vitro* (Jensen & Parmar, 2006; Zhou et al., 2016). The ND1-transduced astrocytes express both the astrocytes GFAP protein as well as neuronal Tuj1 protein, further, aggregate into a neurosphere-like structure, suggesting that these are reprogrammed astrocytes in the

intermediate transition stage. While Guo et al. (2014) proposed that ND1 can induce direct transdifferentiation from astrocytes to neurons, the results observed in the *in vitro* system suggest that at least some of the reprogrammed astrocytes are first reverting back to an immature precursor stage, indicated by the co-expression of astrocyte GFAP and neuronal Tuj1 protein. An intermediate transition stage in reprogramming has been observed in the *in vitro* reprogramming studies using the SOX2 transcription factor (Corti et al., 2012; Heinrich et al., 2014; Niu et al., 2013). This effect could be unique to the *in vitro* system. The difference in environmental cues between the *in vitro* and *in vivo* system may play an important role in defining the trajectories of ND1-driven reprogramming. Grande et al (2013) suggested a crucial role for environmental cues to enhance reprogramming *in vivo*. This limitation of the *in vitro* system is particularly highlighted by the poor AAV transduction efficiency of astrocytes and the low frequency of reprogramming obtained. Future experiments will aim to recapitulate this phenomenon by optimizing multiple aspects of the culture system, which includes astrocyte seeding density and viral titers for transduction.

A few crucial limitations of the *in vitro* reprogramming system are highlighted in the study. First, establishing a pure astrocyte culture system is key to track ND1-mediated fate change. The presence of developing or immature neurons, as observed by Tuj1+ cells in the culture, adds to the complications in interpreting the results of reprogramming *in-vitro*. However, Tuj1+ neuron with reporter mRuby2 expression provides additional evidence of the ability of the AAV9 dual virus system to target neurons. Importantly, a crucial step is to eliminate neuroglial precursor cells from the culture. Since the developing mouse brain at P0-P4 is enriched for precursor cells at various stages of development (Cai, Kurachi, Shibasaki, Okano-Uchida, & Ishizaki, 2012), it can add to the variability in the *in vitro* system. One possible approach to ensure high astrocyte purity in the culture would be to sort for astrocyte using Fluorescence-Activated Cell Sorting (FACS), or alternatively, purify astrocytes based on an immunopanning method (Foo, 2013).

The GFAP::Cre-mediated expression of reporter tdT *in vivo* highlights basic questions regarding the stringency of reporter tdT expression. Random recombination of the dual LoxP sites and inversion of the DIO sequence in the absence of Cre can induce the reporter

expression in non-specific tissues, and results in a mosaic expression pattern (Mao, Fujiwara, & Orkin, 1999). The lack of such mosaic pattern in the intracranial and intravenous delivery model in the brain as well as peripheral tissues supports the hypothesis of the Cre-dependent expression of tdT. However, IHC-analysis for the co-expression of Cre recombinase and tdT will be a crucial validation to be performed. Additionally, tdT expression in wild type Ai9-tdT mouse brains and peripheral tissues will need to be assessed in order to confirm the specificity of tdT expression.

Alternatively, if the tdT expression in the mature resident neurons is indeed Cre-dependent, it poses many interesting questions. This implies some level of activity of the AAV9 plasmid GFAP promoter in mature neurons. Traditionally, active GFAP promoter has been associated with radial glial precursor cells and reactive astrocytes in the adult brain. Interestingly, a study conducted by Hol et al. (2003) delves into the nuances of the GFAP expression observed in mature neurons in patients affected by Alzheimer's disease (AD) and Down Syndrome. Using *in-situ* analysis, the study demonstrates a splice variant of GFAP mRNA is expressed in human hippocampal neurons in disease conditions (Hol et al., 2003). Comparing the results of Hol and colleagues with the GFAP::Cre characterization results obtained in the current study, it is possible that the AAV-9 system is preferentially targeting the resident neurons that possess low-level GFAP promoter activity that is triggered by brain injury. The limited expression of AAV9-GFAP::Cre in neurons in the intravenous delivery model align with this hypothesis, as minimal Cre-driven tdT+ cells were observed in the absence of injury. Retroviral-based vectors fail to target the post-mitotic neurons, thus this observation was not reported in the previous studies. It is possible that the GFAP promoter activity in neurons is due to the episomal expression of the AAV9 constructs. How the activity of the endogenous neuronal GFAP promoter is affected poses an interesting future direction.

The efficiency of the intravenous-delivered AAV-9 to transduce striatal cells was observed to be limited. However, the protocol followed in this study was based on the methodologies adopted from a previous study, published by Foust et al. (2009). They demonstrated that the intravenous delivery of AAV-9 targeted astrocytes targeted caudal regions of the brain i.e. midbrain, hindbrain, and the cerebellum. Thus, characterizing tdT

expression in these regions will be key to validate the success of the AAV-9 intravenous delivery mode. Additionally, they reported the differential effect of viral dosage on the AAV-9 transduction efficiency. Limited transduction efficiency was observed at a low viral dose of 10^{11} GC, but at a viral titer of 10^{12} GC, a ten-fold increase, a substantial infection was observed. Intravenous delivery of higher viral titers of the AAV-9 can provide insight into the concentration-dependent transduction efficiency of the AAV-9.

The lack of GFAP expression in astrocytes in the homeostatic, non-injured brain, as observed in the intravenous AAV-9 delivery model, adds another challenge to analyze reprogramming *in vivo*. Thus additional reliable astrocyte markers will need to be established for analysis of non-injured brains. A theory explaining this result is the sub-threshold expression of GFAP protein in homeostatic astrocytes in a non-injured brain, thus, limiting its detection by IHC. This indicates the potential restricted application of GFAP as a pan astrocyte-specific protein marker in a non-injured brain. Quantification of astrocyte expression of viral constructs would require using ubiquitous astrocyte markers such as S100 calcium-binding protein (S100β) may provide a better strategy to localize astrocytes in a non-perturbed brain.

A recent study by (Chen et al., 2019) interrogated ND1-mediated direct reprogramming in an ischemic stroke model, using a similar AAV-9 dual virus gene delivery strategy employed in this study. The GFAP-driven Cre and CAG-driven ND1, encoded on separate constructs, were demonstrated to convert cortical astrocytes to glutamatergic neurons *in vivo.* In addition, the reprogrammed neurons were shown to replace the neuronal fiber tracts of neurons lost in the injury that recapitulate the same synaptic connections as present before injury. Surprisingly, they reported minimal expression of AAV-9 constructs (~10%) in resident cortical neurons, indicating low GFAP-driven Cre activity in injured neurons. This implicated GFAP promoter activity in injured neurons seems consistent with the GFAP expression observed in mature neurons in the context of AD, as reported by Hol et al. (2003) discussed above. Together, this poses a few interesting questions. (1) Is the GFAP promoter activity, that is otherwise repressed, switched ON in mature resident neurons in the context of injury? (2) Can this biological profile of GFAP promoter activity in mature neurons be exploited to promote ND1-mediated neuronal repair in addition to

targeting reprogramming in the context of injury or neurodegenerative diseases? If so, this would open up novel avenues of investigation to directly target injured neurons to prevent their degeneration.

Future experiments will aim to address AAV-9 cell-type tropism as well as GFAP-promoter expression. Using tissue-specific promoters to drive the expression of the transgene can limit the off-target effects. Chen et al. (2019) report a limited neuronal targeting using a truncated sequence of the human GFAP promoter. Following a similar strategy to limit the AAV9-GFAP::Cre expression to astrocytes, modified GFAP promoter sequences derived either from human or mouse, and the complete and truncated GFAP sequences will be assessed for the specificity of activity in astrocytes. However, identifying such promoters with exclusive specificity poses a great challenge.

In addition, a second approach to validate GFAP promoter activity in astrocytes and neurons will need to be assessed by the delivery of the CAG::mRuby2 reporter construct alone in a GFAP-Cre mouse strain. A consistent observation noted in the *in vivo* experiments in the current study is the limited targeting of striatal astrocytes. It is possible that the striatal astrocytes are amenable to be transduced by other serotypes of AAV compared to the AAV-9. (Hammond, Leek, Richman, & Tjalkens, 2017) demonstrate the superior ability of the serotype AAV-DJ8 to target astrocytes in mixed glial cultures as well as *in vivo* when delivered through the intracerebroventricular route. Using this strategy to target striatal astrocytes in our system is a potential avenue to be explored.

ND1-driven reprogramming in the 6-OHDA Parkinson's disease (PD) mouse model presented interesting results. The Control dual virus system in mouse is predominantly expressed in cortical neuronal cells around the site of injury in the virus-alone experiments. In contrast, the Control virus system injected in the PD model shows successful expression, restricted predominantly to astrocytes. In the AAV9-ND1 overexpressing conditions, viral construct expression was observed in neurons in the vicinity of the injection site. Taken together with previous results, the expression of the AAV9 constructs in mature neurons was anticipated. Surprisingly, viral constructs were also expressed in neurons that did not co-label for mature neuronal protein markers, suggesting that these are potentially reprogrammed neurons, in the early stage of maturation. These cells also show a different

morphology, with bigger cell soma and a single process extending dorsally. Compared to the mRuby+/NeuN+ resident neurons, the mRuby+ neurons had additional tiny processes extending from the cell soma in multiple directions in a haphazard fashion, This suggests that these cells were bona fide reprogrammed cells in the transition state. This was an exciting and contrasting effect seen between the control and ND1-reprogramming condition. Future experiments will aim to validate the expression of ND1 using IHC as well as increase experimental biological replicates to examine the robustness of this system. Additionally, a crucial factor to interrogate is the viral construct expression in the control and ND1-reprogramming condition at a shorter time point, possibly day 1-2 after viral injection. This will provide insight into the AAV-9 targeting patterns as well as to trace the dynamics of reprogramming.

The GFAP promoter activity observed in astrocyte and neurons in the adult brain can serve twofold goals in the context of neurodegenerative diseases, such as Parkinson's disease, where progressive neuronal cell degeneration and death is observed. First, GFAP-driven forced expression of ND1 in the reactive astrocytes in the diseased brain can be targeted for direct neuronal reprogramming to replenish neuronal populations lost due to disease pathology. These neuronal populations include dopaminergic neurons, glutamatergic neurons, and striatal GABAergic neurons. Second, GFAP-driven expression of ND1 can be targeted to resident neurons for repair. We hypothesize that ND1 in injured/stressed resident neurons will initiate transcription factor cascades required for the neuronal developmental program. This in turn could drive the neuron towards a pro-survival and repair mode in the context of PD. This potential two-fold approach offers a therapeutic intervention in the advanced stages of the disease, which is characterized by irreversible neuronal loss. In summary, this study examines the novel and clinically translatable approach of AAV-based delivery of the proneural transcription factor NeuroD1 to drive direct neuronal reprogramming in Parkinson's disease mouse model. The pilot data demonstrated in the current study suggest the potential for developing an AAV-based therapeutic approach to neuronal repair and recovery, thus, targeting functional restoration in human Parkinson's disease.

BIBLIOGRAPHY

Andræ, J., Bongcam-Rudloff, E., Hansson, I., Lendahl, U., Westermark, B., & Nistér, M. (2001). A 1.8 kb GFAP-promoter fragment is active in specific regions of the embryonic CNS. *Mechanisms of Development*, *107*(1–2), 181–185. https://doi.org/10.1016/S0925-4773(01)00460-9

Aschauer, D. F., Kreuz, S., & Rumpel, S. (2013). Analysis of transduction efficiency, tropism and axonal transport of AAV serotypes 1, 2, 5, 6, 8 and 9 in the mouse brain. *PloS One*, *8*(9), e76310–e76310. https://doi.org/10.1371/journal.pone.0076310

Atasoy, D., Aponte, Y., Su, H. H., & Sternson, S. M. (2008). A FLEX Switch Targets Channelrhodopsin-2 to Multiple Cell Types for Imaging and Long-Range Circuit Mapping. *The Journal of Neuroscience*, *28*(28), 7025 LP – 7030. https://doi.org/10.1523/JNEUROSCI.1954-08.2008

Barker, R. A., Barrett, J., Mason, S. L., & Björklund, A. (2013). Fetal dopaminergic transplantation trials and the future of neural grafting in Parkinson's disease. *The Lancet Neurology*, *12*(1), 84–91. https://doi.org/10.1016/S1474-4422(12)70295-8

Baum, C. (2007). Insertional mutagenesis in gene therapy and stem cell biology. *Current Opinion in Hematology*, *14*(4). Retrieved from https://journals.lww.com/co-hematology/Fulltext/2007/07000/Insertional_mutagenesis_in_gene_therapy_and_stem.6.aspx

Best, B. P. (2015). Cryoprotectant Toxicity: Facts, Issues, and Questions. *Rejuvenation Research*, *18*(5), 422–436. https://doi.org/10.1089/rej.2014.1656

Boenisch, T. (2001). Formalin-Fixed and Heat-Retrieved Tissue Antigens: A Comparison of Their Immunoreactivity in Experimental Antibody Diluents. *Applied Immunohistochemistry & Molecular Morphology*, *9*(2). Retrieved from https://journals.lww.com/appliedimmunohist/Fulltext/2001/06000/Formalin_Fixed_and_Heat_Retrieved_Tissue_Antigens_.11.aspx

Brown, P. O., Bowerman, B., Varmus, H. E., & Bishop, J. M. (1987). Correct integration of retroviral DNA in vitro. *Cell*, *49*(3), 347–356. https://doi.org/10.1016/0092-8674(87)90287-X

Bundy, H. F., & Mehl, J. W. (1959). Trypsin Inhibitors of Human Serum: II. ISOLATION OF THE α1-INHIBITOR AND ITS PARTIAL CHARACTERIZATION . *Journal of Biological Chemistry* , *234*(5), 1124–1128. Retrieved from http://www.jbc.org/content/234/5/1124.short

Cai, N., Kurachi, M., Shibasaki, K., Okano-Uchida, T., & Ishizaki, Y. (2012). CD44-Positive Cells Are Candidates for Astrocyte Precursor Cells in Developing Mouse Cerebellum. *The Cerebellum*, *11*(1), 181–193. https://doi.org/10.1007/s12311-011-0294-x

Caiazzo, M., Dell'Anno, M. T., Dvoretskova, E., Lazarevic, D., Taverna, S., Leo, D., … Broccoli, V. (2011). Direct generation of functional dopaminergic neurons from mouse and human fibroblasts. *Nature*, *476*(7359), 224–227. https://doi.org/10.1038/nature10284

Chen, Y.-C., Ma, N.-X., Pei, Z.-F., Wu, Z., Do-Monte, F. H., Keefe, S., … Chen, G. (2019a). A NeuroD1 AAV-Based Gene Therapy for Functional Brain Repair after Ischemic Injury through In Vivo Astrocyte-to-Neuron Conversion. *Molecular Therapy*.

https://doi.org/10.1016/j.ymthe.2019.09.003

Chen, Y.-C., Ma, N.-X., Pei, Z.-F., Wu, Z., Do-Monte, F. H., Keefe, S., … Chen, G. (2019b). A NeuroD1 AAV-Based Gene Therapy for Functional Brain Repair after Ischemic Injury through In Vivo Astrocyte-to-Neuron Conversion. *Molecular Therapy : The Journal of the American Society of Gene Therapy*, *0*(0). https://doi.org/10.1016/j.ymthe.2019.09.003

Chinta, S. J., & Andersen, J. K. (2005). Dopaminergic neurons. *The International Journal of Biochemistry & Cell Biology*, *37*(5), 942–946. https://doi.org/10.1016/J.BIOCEL.2004.09.009

Cho, J., & Tsai, M. (2004). *The Role of BETA2 / NeuroD1 in the Development*. *30*(1), 35–47.

Corti, S., Nizzardo, M., Simone, C., Falcone, M., Donadoni, C., Salani, S., … Comi, G. P. (2012). Direct reprogramming of human astrocytes into neural stem cells and neurons. *Experimental Cell Research*, *318*(13), 1528–1541. https://doi.org/10.1016/j.yexcr.2012.02.040

Dai, J., Bercury, K. K., Ahrendsen, J. T., & Macklin, W. B. (2015). Olig1 function is required for oligodendrocyte differentiation in the mouse brain. *The Journal of Neuroscience : The Official Journal of the Society for Neuroscience*, *35*(10), 4386–4402. https://doi.org/10.1523/JNEUROSCI.4962-14.2015

Deyle, D. R., & Russell, D. W. (2009). Adeno-associated virus vector integration. *Current Opinion in Molecular Therapeutics*, *11*(4), 442–447. Retrieved from http://www.ncbi.nlm.nih.gov/pubmed/19649989%0Ahttp://www.pubmedcentral.nih.gov/articlerender.fcgi?artid=PMC2929125

Du, F., Qian, Z. M., Zhu, L., Wu, X. M., Qian, C., Chan, R., & Ke, Y. (2010). Purity, cell viability, expression of GFAP and bystin in astrocytes cultured by different procedures. *Journal of Cellular Biochemistry*, *109*(1), 30–37. https://doi.org/10.1002/jcb.22375

Eddleston, M., & Mucke, L. (1993). Molecular profile of reactive astrocytes—Implications for their role in neurologic disease. *Neuroscience*, *54*(1), 15–36. https://doi.org/10.1016/0306-4522(93)90380-X

Ellis, B. L., Hirsch, M. L., Barker, J. C., Connelly, J. P., Steininger, R. J., & Porteus, M. H. (2013). A survey of ex vivo/in vitro transduction efficiency of mammalian primary cells and cell lines with Nine natural adeno-associated virus (AAV1-9) and one engineered adeno-associated virus serotype. *Virology Journal*, *10*, 1–10. https://doi.org/10.1186/1743-422X-10-74

Eng, L. F., Vanderhaeghen, J. J., Bignami, A., & Gerstl, B. (1971). An acidic protein isolated from fibrous astrocytes. *Brain Research*, *28*(2), 351–354. https://doi.org/10.1016/0006-8993(71)90668-8

Fischer, A. H., Jacobson, K. A., Rose, J., & Zeller, R. (2008). Cryosectioning Tissues. *Cold Spring Harbor Protocols* , *2008*(8), pdb.prot4991. https://doi.org/10.1101/pdb.prot4991

Foo, L. C. (2013). Purification of Rat and Mouse Astrocytes by Immunopanning. *Cold Spring Harbor Protocols* , *2013*(5), pdb.prot074211. https://doi.org/10.1101/pdb.prot074211

Foust, K. D., Nurre, E., Montgomery, C. L., Hernandez, A., Chan, C. M., & Kaspar, B. K. (2009). Intravascular AAV9 preferentially targets neonatal neurons and adult astrocytes. *Nature Biotechnology*, *27*(1), 59–65. https://doi.org/10.1038/nbt.1515

Gage, G. J., Kipke, D. R., & Shain, W. (2012). Whole animal perfusion fixation for rodents. *Journal of Visualized Experiments : JoVE*, (65), 3564. https://doi.org/10.3791/3564

Gao, G., & Wilson, L. H. V. and J. M. (2005). New Recombinant Serotypes of AAV Vectors. *Current Gene Therapy*, Vol. 5, pp. 285–297. https://doi.org/http://dx.doi.org/10.2174/1566523054065057

Gao, Z., Ure, K., Ables, J. L., Lagace, D. C., Nave, K.-A., Goebbels, S., … Hsieh, J. (2009). Neurod1 is essential for the survival and maturation of adult-born neurons. *Nature Neuroscience*, *12*(9), 1090–1092. https://doi.org/10.1038/nn.2385

Gascón, S., Masserdotti, G., Russo, G. L., & Götz, M. (2017). Direct Neuronal Reprogramming: Achievements, Hurdles, and New Roads to Success. *Cell Stem Cell*. https://doi.org/10.1016/j.stem.2017.06.011

Goldman, S. A. (2016). Stem and Progenitor Cell-Based Therapy of the Central Nervous System: Hopes, Hype, and Wishful Thinking. *Cell Stem Cell*, *18*(2), 174–188. https://doi.org/10.1016/j.stem.2016.01.012

Goldman, S. A., Zukhar, A., Barami, K., Mikawa, T., & Niedzwiecki, D. (1996). Ependymal/subependymal zone cells of postnatal and adult songbird brain generate both neurons and nonneuronal siblings in vitro and in vivo. *Journal of Neurobiology*, *30*(4), 505–520. https://doi.org/10.1002/(SICI)1097-4695(199608)30:4<505::AID-NEU6>3.0.CO;2-7

Grande, A., Sumiyoshi, K., López-Juárez, A., Howard, J., Sakthivel, B., Aronow, B., … Nakafuku, M. (2013). Environmental impact on direct neuronal reprogramming in vivo in the adult brain. *Nature Communications*, *4*. https://doi.org/10.1038/ncomms3373

Griffin, J. M., Fackelmeier, B., Fong, D. M., Mouravlev, A., Young, D., & O'Carroll, S. J. (2019). Astrocyte-selective AAV gene therapy through the endogenous GFAP promoter results in robust transduction in the rat spinal cord following injury. *Gene Therapy*, *26*(5), 198–210. https://doi.org/10.1038/s41434-019-0075-6

Guo, Z., Zhang, L., Wu, Z., Chen, Y., Wang, F., & Chen, G. (2014). In vivo direct reprogramming of reactive glial cells into functional neurons after brain injury and in an Alzheimer's disease model. *Cell Stem Cell*, *14*(2), 188–202. https://doi.org/10.1016/j.stem.2013.12.001

Hammond, S. L., Leek, A. N., Richman, E. H., & Tjalkens, R. B. (2017). Cellular selectivity of AAV serotypes for gene delivery in neurons and astrocytes by neonatal intracerebroventricular injection. *PloS One*, *12*(12), e0188830–e0188830. https://doi.org/10.1371/journal.pone.0188830

Heinrich, C., Bergami, M., Gascón, S., Lepier, A., Viganò, F., Dimou, L., … Götz, M. (2014). Sox2-mediated conversion of NG2 glia into induced neurons in the injured adult cerebral cortex. *Stem Cell Reports*, *3*(6), 1000–1014. https://doi.org/10.1016/j.stemcr.2014.10.007

Higashimoto, T., Urbinati, F., Perumbeti, A., Jiang, G., Zarzuela, A., Chang, L. J., … Malik, P. (2007). The woodchuck hepatitis virus post-transcriptional regulatory element reduces readthrough transcription from retroviral vectors. *Gene Therapy*, *14*(17), 1298–1304. https://doi.org/10.1038/sj.gt.3302979

Hol, E. M., Roelofs, R. F., Moraal, E., Sonnemans, M. A. F., Sluijs, J. A., Proper, E. A., … van Leeuwen, F. W. (2003). Neuronal expression of GFAP in patients with Alzheimer pathology and identification of novel GFAP splice forms. *Molecular Psychiatry*, *8*(9), 786–

796. https://doi.org/10.1038/sj.mp.4001379

Hu, W., Qiu, B., Guan, W., Wang, Q., Wang, M., Li, W., … Pei, G. (2015). Direct Conversion of Normal and Alzheimer's Disease Human Fibroblasts into Neuronal Cells by Small Molecules. *Cell Stem Cell*, *17*(2), 204–212. https://doi.org/10.1016/J.STEM.2015.07.006

Jang, T. H., Park, S. C., Yang, J. H., Kim, J. Y., Seok, J. H., Park, U. S., … Han, J. (2017). Cryopreservation and its clinical applications. *Integrative Medicine Research*, *6*(1), 12–18. https://doi.org/10.1016/j.imr.2016.12.001

Jensen, J. B., & Parmar, M. (2006). Strengths and limitations of the neurosphere culture system. *Molecular Neurobiology*, *34*(3), 153–161. https://doi.org/10.1385/MN:34:3:153

Korzhevskii, D. E., & Kirik, O. V. (2016). Brain Microglia and Microglial Markers. *Neuroscience and Behavioral Physiology*, *46*(3), 284–290. https://doi.org/10.1007/s11055-016-0231-z

Ladewig, J., Mertens, J., Kesavan, J., Doerr, J., Poppe, D., Glaue, F., … Brüstle, O. (2012). Small molecules enable highly efficient neuronal conversion of human fibroblasts. *Nature Methods*, *9*(6), 575–578. https://doi.org/10.1038/nmeth.1972

Lee, J. E., Hollenberg, S. M., Snider, L., Turner, D. L., Lipnick, N., & Weintraub, H. (1995). Conversion of Xenopus ectoderm into neurons by neuroD, a basic helix-loop-helix protein. *Science*, *268*(5212), 836–844. https://doi.org/10.1126/science.7754368

Lee, Y., Messing, A., Su, M., & Brenner, M. (2008). GFAP promoter elements required for region-specific and astrocyte-specific expression. *Glia*, *56*(5), 481–493. https://doi.org/10.1002/glia.20622

Lewis, S. A., Balcarek, J. M., Krek, V., Shelanski, M., & Cowan, N. J. (1984). Sequence of a cDNA clone encoding mouse glial fibrillary acidic protein: structural conservation of intermediate filaments. *Proceedings of the National Academy of Sciences of the United States of America*, *81*(9), 2743–2746. https://doi.org/10.1073/pnas.81.9.2743

Li, X., Zuo, X., Jing, J., Ma, Y., Wang, J., Liu, D., … Deng, H. (2015). Small-Molecule-Driven Direct Reprogramming of Mouse Fibroblasts into Functional Neurons. *Cell Stem Cell*, *17*(2), 195–203. https://doi.org/10.1016/J.STEM.2015.06.003

Liddelow, S. A., & Barres, B. A. (2017). Reactive Astrocytes: Production, Function, and Therapeutic Potential. *Immunity*, *46*(6), 957–967. https://doi.org/10.1016/j.immuni.2017.06.006

Liddelow, S. A., Guttenplan, K. A., Clarke, L. E., Bennett, F. C., Bohlen, C. J., Schirmer, L., … Barres, B. A. (2017). Neurotoxic reactive astrocytes are induced by activated microglia. *Nature*, *541*(7638), 481–487. https://doi.org/10.1038/nature21029

Liu, M., Pereira, F. A., Price, S. D., Chu, M. J., Shope, C., Himes, D., … Tsai, M. J. (2000). Essential role of BETA2/NeuroD1 in development of the vestibular and auditory systems. *Genes and Development*, *14*(22), 2839–2854. https://doi.org/10.1101/gad.840500

Liu, Y., Miao, Q., Yuan, J., Han, S., Zhang, P., Li, S., … Cheng, L. (2015). Ascl1 Converts Dorsal Midbrain Astrocytes into Functional Neurons In Vivo. *Journal of Neuroscience*, *35*(25). https://doi.org/10.1523/JNEUROSCI.3975-14.2015

Loeb, J. E., Cordier, W. S., Harris, M. E., Weitzman, M. D., & Hope, T. J. (1999). Enhanced Expression of Transgenes from Adeno-Associated Virus Vectors with the Woodchuck

Hepatitis Virus Posttranscriptional Regulatory Element: Implications for Gene Therapy. *Human Gene Therapy*, *10*(14), 2295–2305. https://doi.org/10.1089/10430349950016942

Lykken, E. A., Shyng, C., Edwards, R. J., Rozenberg, A., & Gray, S. J. (2018). Recent progress and considerations for AAV gene therapies targeting the central nervous system. *Journal of Neurodevelopmental Disorders*, *10*(1), 16. https://doi.org/10.1186/s11689-018-9234-0

Ma, Q., Kintner, C., & Anderson, D. J. (1996). Identification of neurogenin, a vertebrate neuronal determination gene. *Cell*, Vol. 87, pp. 43–52. https://doi.org/10.1016/S0092-8674(00)81321-5

Mao, X., Fujiwara, Y., & Orkin, S. H. (1999). Improved reporter strain for monitoring Cre recombinase-mediated DNA excisions in mice. *Proceedings of the National Academy of Sciences of the United States of America*, *96*(9), 5037–5042. https://doi.org/10.1073/pnas.96.9.5037

Margolesky, J., & Singer, C. (2018). Extended-release oral capsule of carbidopa–levodopa in Parkinson disease. *Therapeutic Advances in Neurological Disorders*, *11*, 1756285617737728.

Matsuda, T., Irie, T., Katsurabayashi, S., Hayashi, Y., Nagai, T., & Hamazaki, N. (2019). Pioneer Factor NeuroD1 Rearranges Transcriptional and Epigenetic Profiles to Execute Microglia-Neuron Article Pioneer Factor NeuroD1 Rearranges Transcriptional and Epigenetic Profiles to Execute Microglia-Neuron Conversion. *Neuron*, *101*(3), 472-485.e7. https://doi.org/10.1016/j.neuron.2018.12.010

Mazia, D., Schatten, G., & Sale, W. (1975). Adhesion of cells to surfaces coated with polylysine. Applications to electron microscopy. *The Journal of Cell Biology*, *66*(1), 198–200. https://doi.org/10.1083/jcb.66.1.198

McCarty, D. M., Young, S. M., & Samulski, R. J. (2004). Integration of Adeno-Associated Virus (AAV) and Recombinant AAV Vectors. *Annual Review of Genetics*, *38*(1), 819–845. https://doi.org/10.1146/annurev.genet.37.110801.143717

Merkel, S. F., Andrews, A. M., Lutton, E. M., Mu, D., Hudry, E., Hyman, B. T., … Ramirez, S. H. (2017). Trafficking of adeno-associated virus vectors across a model of the blood-brain barrier; a comparative study of transcytosis and transduction using primary human brain endothelial cells. *Journal of Neurochemistry*, *140*(2), 216–230. https://doi.org/10.1111/jnc.13861

Nagatsu, T., & Sawada, M. (2009). L-dopa therapy for Parkinson's disease: Past, present, and future. *Parkinsonism & Related Disorders*, *15*, S3–S8. https://doi.org/10.1016/S1353-8020(09)70004-5

Naldini, L. (1998). Lentiviruses as gene transfer agents for delivery to non-dividing cells. *Current Opinion in Biotechnology*, *9*(5), 457–463. https://doi.org/10.1016/S0958-1669(98)80029-3

Naso, M. F., Tomkowicz, B., Perry 3rd, W. L., & Strohl, W. R. (2017). Adeno-Associated Virus (AAV) as a Vector for Gene Therapy. *BioDrugs : Clinical Immunotherapeutics, Biopharmaceuticals and Gene Therapy*, *31*(4), 317–334. https://doi.org/10.1007/s40259-017-0234-5

Niu, W., Zang, T., Zou, Y., Fang, S., Smith, D. K., Bachoo, R., & Zhang, C. L. (2013). In vivo reprogramming of astrocytes to neuroblasts in the adult brain. *Nature Cell Biology*, *15*(10), 1164–1175. https://doi.org/10.1038/ncb2843

Notman, R., Noro, M., O'Malley, B., & Anwar, J. (2006). Molecular Basis for Dimethylsulfoxide (DMSO) Action on Lipid Membranes. *Journal of the American Chemical Society*, *128*(43), 13982–13983. https://doi.org/10.1021/ja063363t

Oberheim, N. A., Goldman, S. A., Nedergaard, M., Heinrich, C., Götz, M., & Berninger, B. (2012). Heterogeneity of astrocytic form and function. *Methods in Molecular Biology (Clifton, N.J.)*, *814*, 23–45. https://doi.org/10.1007/978-1-61779-452-0_3

Ohsawa, K., Imai, Y., Sasaki, Y., & Kohsaka, S. (2004). Microglia/macrophage-specific protein Iba1 binds to fimbrin and enhances its actin-bundling activity. *Journal of Neurochemistry*, *88*(4), 844–856. https://doi.org/10.1046/j.1471-4159.2003.02213.x

Parkinson, J. (2002). An essay on the shaking palsy. *The Journal of Neuropsychiatry and Clinical Neurosciences*, *14*(2), 223–236.

Pataskar, A., Jung, J., Smialowski, P., Noack, F., Calegari, F., Straub, T., & Tiwari, V. K. (2016). *factor landscapes to induce the neuronal program*. *35*(1).

Paxinos, G., & Watson, C. (2006). *The rat brain in stereotaxic coordinates: hard cover edition*. Elsevier.

Rivetti Di Val Cervo, P., Romanov, R. A., Spigolon, G., Masini, D., Martín-Montañez, E., Toledo, E. M., … Arenas, E. (2017). Induction of functional dopamine neurons from human astrocytes in vitro and mouse astrocytes in a Parkinson's disease model. *Nature Biotechnology*, *35*(5), 444–452. https://doi.org/10.1038/nbt.3835

Schebesta, M., & Serluca, F. C. (2009). olig1 expression identifies developing oligodendrocytes in zebrafish and requires hedgehog and notch signaling. *Developmental Dynamics*, *238*(4), 887–898. https://doi.org/10.1002/dvdy.21909

Schildge, S., Bohrer, C., Beck, K., & Schachtrup, C. (2013). Isolation and culture of mouse cortical astrocytes. *Journal of Visualized Experiments : JoVE*, (71), 50079. https://doi.org/10.3791/50079

Schnepp, B. C., Jensen, R. L., Chen, C.-L., Johnson, P. R., & Clark, K. R. (2005). Characterization of adeno-associated virus genomes isolated from human tissues. *Journal of Virology*, *79*(23), 14793–14803. https://doi.org/10.1128/JVI.79.23.14793-14803.2005

Schuster, D. J., Dykstra, J. A., Riedl, M. S., Kitto, K. F., Belur, L. R., Scott McIvor, R., … Vulchanova, L. (2014). Biodistribution of adeno-associated virus serotype 9 (AAV9) vector after intrathecal and intravenous delivery in mouse. *Frontiers in Neuroanatomy*, *8*(JUN), 1–14. https://doi.org/10.3389/fnana.2014.00042

Shibata, T., Yamada, K., Watanabe, M., Ikenaka, K., Wada, K., Tanaka, K., & Inoue, Y. (1997). Glutamate Transporter GLAST Is Expressed in the Radial Glia–Astrocyte Lineage of Developing Mouse Spinal Cord. *The Journal of Neuroscience*, *17*(23), 9212 LP – 9219. https://doi.org/10.1523/JNEUROSCI.17-23-09212.1997

Soltis, R. D., Hasz, D., Morris, M. J., & Wilson, I. D. (1979). The effect of heat inactivation of serum on aggregation of immunoglobulins. *Immunology*, *36*(1), 37–45. Retrieved from https://www.ncbi.nlm.nih.gov/pubmed/422227

Takahashi, K., & Yamanaka, S. (2006). Induction of Pluripotent Stem Cells from Mouse Embryonic and Adult Fibroblast Cultures by Defined Factors. *Cell*, *126*(4), 663–676. https://doi.org/10.1016/J.CELL.2006.07.024

Tieu, K. (2011). A guide to neurotoxic animal models of Parkinson's disease. *Cold Spring Harbor Perspectives in Medicine*, *1*(1), a009316–a009316. https://doi.org/10.1101/cshperspect.a009316

Trichas, G., Begbie, J., & Srinivas, S. (2008). Use of the viral 2A peptide for bicistronic expression in transgenic mice. *BMC Biology*, *6*, 40. https://doi.org/10.1186/1741-7007-6-40

Triglia, R. P., & Linscott, W. D. (1980). Titers of nine complement components, conglutinin and C3b-inactivator in adult and fetal bovine sera. *Molecular Immunology*, *17*(6), 741–748. https://doi.org/10.1016/0161-5890(80)90144-3

Virchow, R. (1855). Ein Fall von progressiver Muskelatrophie. *Archiv für Pathologische Anatomie und Physiologie und für Klinische Medicin*, *8*(4), 537–540. https://doi.org/10.1007/BF01936110

Waddington, C. H. (2014). *The strategy of the genes*. Routledge.

Warnock, J. N., Daigre, C., & Al-Rubeai, M. (2011). *Introduction to Viral Vectors BT - Viral Vectors for Gene Therapy: Methods and Protocols* (O.-W. Merten & M. Al-Rubeai, Eds.). https://doi.org/10.1007/978-1-61779-095-9_1

Yokoyama, W. M., Thompson, M. L., & Ehrhardt, R. O. (2012). Cryopreservation and Thawing of Cells. *Current Protocols in Immunology*, *99*(1), A.3G.1-A.3G.5. https://doi.org/10.1002/0471142735.ima03gs99

Yu, P., Wang, H., Katagiri, Y., & Geller, H. M. (2012). An in vitro model of reactive astrogliosis and its effect on neuronal growth. *Methods in Molecular Biology (Clifton, N.J.)*, *814*, 327–340. https://doi.org/10.1007/978-1-61779-452-0_21

Zamanian, J. L., Xu, L., Foo, L. C., Nouri, N., Zhou, L., Giffard, R. G., & Barres, B. A. (2012). Genomic Analysis of Reactive Astrogliosis. *The Journal of Neuroscience*, *32*(18), 6391 LP – 6410. https://doi.org/10.1523/JNEUROSCI.6221-11.2012

Zhang, H., Yang, B., Mu, X., Ahmed, S. S., Su, Q., He, R., … Gao, G. (2011). Several rAAV vectors efficiently cross the blood-brain barrier and transduce neurons and astrocytes in the neonatal mouse central nervous system. *Molecular Therapy : The Journal of the American Society of Gene Therapy*, *19*(8), 1440–1448. https://doi.org/10.1038/mt.2011.98

Zhou, S., Szczesna, K., Ochalek, A., Kobolák, J., Varga, E., Nemes, C., … Avci, H. X. (2016). Neurosphere Based Differentiation of Human iPSC Improves Astrocyte Differentiation. *Stem Cells International*, *2016*, 4937689. https://doi.org/10.1155/2016/4937689

Zincarelli, C., Soltys, S., Rengo, G., & Rabinowitz, J. E. (2008). Analysis of AAV serotypes 1-9 mediated gene expression and tropism in mice after systemic injection. *Molecular Therapy*, Vol. 16, pp. 1073–1080. https://doi.org/10.1038/mt.2008.76

APPENDIX I: List of Abbreviations

6-OHDA – 6-hydroxydopamine

AAV – Adeno-Associated Virus

BSA – Bovine Serum Albumin

BBB – Blood-Brain Barrier

CAG – Cytomegalus Virus (CMV) enhancer fused to Chicken β-Actin promoter

CNS – Central Nervous System

DAPI - 4′, 6-diamidino-2-phenylindole

DIO – Double-Inverted Flox

DMSO – Dimethyl sulfoxide

DMEM – Dulbecco's Modified Eagle Media

FBS – Fetal Bovine Serum

GFAP – Glial Fibrillary Acidic protein

HBSS – Hank's Balanced Salt Solution

HS – Horse serum

IHC – Immunohistochemistry

ICC – Immunocytochemistry

L-DOPA – Levodopa

ND1 – NeuroD1

OCT – Optimum Cutting Temperature

PFA – Paraformaldehyde

PD – Parkinson's disease

PBS – Phosphate Buffered Saline

PHT – Phosphate Buffer + Horse serum + Triton

PLL – Poly-L-Lysine

tdT – tdTomato

TFM – Tissue Freezing Medium

WT – Wild Type

APPENDIX II: Viral Titer Calculation for *In vitro* Transduction

1. MOI – Number of viral particles transducing individual cell
2. Total virus titer required = Total number of cells * MOI / Native viral titer
3. Volume of viral solution required = Required No. of viral particles / Native viral titer

A. MOI – 80,000

		AAV	Titer GC/ml	GC/well	AAV/well (µL)
	Exp	AAV9-CAG-DIO-NeuroD1-T2A-mRuby2	1.82E+14	6.40E+09	0.04
Con		AAV9-GFAP-Cre	1.67E+14	6.40E+09	0.04
		AAV9-CAG-DIO-mRuby2	3.15E+14	6.40E+09	0.02
		Working Stock	50x		
		MOI	80,000		
		Cells/well	80,000		
		# of wells	8		
		Volume/well (µl)	300		

Table 5: *AAV-9 working solution viral titer calculation for MOI of 80,000*

GC – Genome Content

AAV for 50x working (µL)	Diluent for 50x Working (µL)	50x to 1x working (µL)	Diluent for 1x working (µL)	Total volume/well (AAV1Diluent1 + AAV2Diluent2)
1.76	48.24	3	147	300
1.92	48.08	3	147	
1.02	48.98	3	147	

Table 6: *Calculation for the AAV-9 stock solution dilution for MOI of 80,000*

B. MOI – 160,000

		AAV	Titer GC/ml	GC/well	AAV/well (µL)
	Exp	AAV9-CAG-DIO-NeuroD1-T2A-mRuby2	1.82E+14	1.28E+10	0.07
Con		AAV9-GFAP-Cre	1.67E+14	1.28E+10	0.08
		AAV9-CAG-DIO-mRuby2	3.15E+14	1.28E+10	0.04
		Working Stock	50x		
		MOI	160,000		
		Cells/well	80,000		
		# of wells	8		
		Volume/well (µl)	300		

Table 7: *AAV-9 working solution viral titer calculation for MOI of 160,000*

GC – Genome Content

AAV for 50x working (µL)	Diluent for 50x Working (µL)	50x to 1x working (µL)	Diluent for 1x working (µL)	Total volume/well (AAV1Diluent1 + AAV2Diluent2)
3.52	46.48	3	147	300
3.83	46.17	3	147	
2.03	47.97	3	147	

Table 8: *Calculation for the AAV-9 stock solution dilution for MOI of 160,000*

APPENDIX III: Antibodies for IHC/ICC

1. Primary Antibodies

Sl. No.	***Protein antibody***	***Host Species/Ig***	***Dilution IHC/ICC***	***Vendor***	***Catalog No.***
1.	EAAT-1 (GLAST)	Rb pAb	1:200	Abcam	ab416
2.	GFAP	Rt pAb	1:500	Lifespan Biosciences	LS-C7076
		Ch pAb	1:500	Lifespan Biosciences	LS-B4775
3.	NeuN	Rb mAb	1:500	Abcam	ab177487
		Ms mAb	1:500	Abcam	ab104224
4.	NeuroD1	Gt pAb	1:200	RnD Systems	AF2746
5.	Olig1	Ms pAb	1:200	RnD Systems	MAB2417
6.	Vimentin	Ms mAb	1:200	DAKO	M7020
7.	Tuj1	Ms	1:1000	BioLegend (Covance)	MMS-435P

Ch – Chicken, Gt – Goat, Ms- Mouse, Rb – Rabbit, Rt – Rat

2. Secondary Antibodies

Sl. No.	***Fluorescent Wavelength***	***Target Species***	***Dilution IHC/ICC***	***Vendor***	***Catalog No.***
1.	**488**	Ch	1:1000	Jackson Immunoresearch	703-545-155
		Ms		Abcam	Ab150105
		Rt		Invitrogen	A21208
		Rb		Abcam	Ab150073
		Gt			Ab150129
2.	**647**	Ch		Jackson Immunoresearch	703-605-155
		Ms		Abcam	Ab150107
		Rt			Ab150155
		Rb			Ab150075
		Gt			Ab150131

All the secondary antibodies were raised in donkey.